The nuclear-deformation surface $\beta(Z,N)$ for nuclei with $Z=2$–102

A. V. Yushkov
Institute of Nuclear Physics, Kazakh Academy of Sciences, Alma-Ata

Fiz. Elem. Chastits At. Yadra **24**, 348–408 (March–April 1993)

Absolute values and signs of the equilibrium quadrupole nuclear deformation have been extracted from experimental data on the scattering of α particles of intermediate energies (20–140 MeV) by means of the coupled-channel method (CCM) and the Blair phase-shift method (BPSM). Comparison of the experimental data with theoretical results calculated in a superfluid model revealed good agreement not only in absolute magnitude but also functional similarity in the coordinates (Z,N). In such calculations, the main role in the isotopic and isotonic dependences $\beta(Z,N)$ is played by the excitation energy of the first 2^+ level in the form $\beta \sim 1/E_{2+}^{*1/2}$; this excitation energy can be measured with very good accuracy in nuclear spectroscopy. The relationship is used in the present paper to obtain the complete experimental $\beta(Z,N)$ surface from experimental data on E_{2+}^{*}, which are known not only for all stable nuclei but also for a large number of radioactive even–even nuclei. Investigation of the deformation surface has revealed some interesting properties, both in the absolute magnitudes of the nuclear deformation and in shape phase transitions of the nuclei. From these properties, conclusions are drawn concerning the possible reasons for the finiteness of the periodic table for stable nuclei and the restricted stability lines for isotopic chains.

1. INTRODUCTION

The shape, composition, and deformation of nuclei are central problems of modern nuclear physics. The theoretical solution of these problems requires the solution of a many-body problem involving questions relating to the choice of the residual interaction and other matters that in principle cannot be solved exactly.[1,2] The resulting difficulties can be eliminated only by comparing the predictions of a theoretical model with the results of an adequate experiment. Therefore, in the framework of the formulated problems we have new problems, and experimental investigations of the equilibrium deformation of nuclei or their deformation in excited states are topical. For individual nuclei that have been studied, it is important to raise the accuracy of the measurements, and for other nuclei or regions of them the systematic accumulation and analysis of new facts are important. However, for the solution of modern problems of nuclear physics, the most important thing is to obtain systematic experimental data, not for individual nuclei, but, for example, for nuclear isotopic chains or for fairly large regions in N and Z.

Practically from the time of discovery of the nucleus[3] spatial and geometrical arguments, initially classical as a rule, were at the forefront in the development of nuclear models. Using geometrical terminology, one can say that the model of a "point nucleus" was the first spatial model of the nucleus,[3] and it indicated unique nuclear properties: large mass, high density, charge, and spatial localization. The experiments of Hofstadter *et al.*[4] finally confirmed the ideas, already existing at that time, of the "ball nucleus" model, and the problem of nuclear geometry entered nuclear physics. Two parameters made their first appearance: the radius R of a nucleus and the thickness ΔR of its surface layer. The problem of nuclear shape, in particular nonsphericity, arose with the creation of the generalized nuclear model of Bohr and Mottelson,[5,6] which can be called the "spheroid nucleus" model. A further spatial nuclear parameter was introduced: the nuclear quadrupole deformation parameter β_2, which by definition is[5,6]

$$\beta_2=\left(\frac{16\pi}{45}\right)^{1/2}\frac{a-b}{R_0}=1.06\,\frac{a-b}{R_0} \tag{1}$$

and occurs in the expression for the nuclear shape:

$$R(\theta)=R_0[1+\beta_2 Y_{20}(\theta,\varphi)], \tag{2}$$

where a and b are the semiaxes of the spheroid, $R_0=1.2A^{1/3}$ is the rms radius of the nucleus, and $Y_{20}(\theta,\varphi)$ is a spherical function.

No one has yet succeeded in measuring directly in an experiment the nuclear quadrupole deformation parameter β_2; it is obtained from the nuclear matrix elements of transitions of the nucleus to excited states: $|C_1(2)|$. In this connection, the most important experiments are the ones sensitive to the spatial details of the nuclear structure. In the first place, there are diffraction experiments, and these include elastic and inelastic scattering of complex particles. The small value of the de Broglie wavelength $\lambda\!\!\!^{-}$ of the incident particle relative to the radius R of the scattering object—a necessary requirement for the realization of nuclear diffraction—not only makes the process highly sensitive to the spatial structure of the nuclear object but also greatly simplifies the determination of the interaction amplitude, even making it possible in a number of cases to find the amplitude in analytic form. This, in its turn, makes it possible to extract β_2 from experiments accurately and quite simply.

A very important aspect of experimental studies of nuclear reactions aimed at measuring β_2 is the choice of ap-

 1063-7796/93/020149-28$10.00

propriate conditions such as the species of incident particles, their energies, the masses of the target nuclei, and the nature of the excited nuclear states. For what one must do is to select a nuclear process in which the interaction is almost entirely due to the wave nature of the interacting nuclear objects and, therefore, their geometry. Thus, among all nuclear reactions the scattering process is distinguished by virtue of the fact that the wave functions in the entrance and exit channels have the same nature and because there exist angle and energy regions of "pure" diffraction interactions. The scattering process became one of the fundamental methods of investigating structure and, in particular, nonsphericity of nuclei.

On the other hand, one of the "eternal" problems of experimental nuclear physics was the desire to relate the results obtained from nuclear reactions to the results of nuclear spectroscopy, since the latter gives record accuracies of measurement of nuclear parameters. In the present paper, it is shown that this could be done with respect to the nuclear quadrupole deformation parameter.

It is true that in both nuclear spectroscopy and nuclear scattering the experimentally obtained parameter β_2 remains essentially a model physical quantity, but the agreement of the absolute values of β_2 obtained by different methods, especially the close similarity of their functional dependences on N and Z, $\beta_2(N)$ and $\beta_2(Z)$, makes these parameters model-independent and adequate descriptions of the physics of nuclear structure.

Given the genuine increase in the accuracy and the reliability of the experimentally determined nuclear quadrupole deformation parameters, one can pose the problem of studying the variation of β_2 in the complete region of existence in Z and N. It is extremely interesting to establish how smoothly the nuclear shape varies with atomic weight, and also to establish the boundaries at which the sign of the deformation changes (oblateness–prolateness effects), i.e., transitions from prolate shape of the nuclear surface ($\text{sign}\,\beta_2 > 0$) to oblate shape ($\text{sign}\,\beta_2 < 0$). These oblate–prolate effects are known in the literature as nuclear shape phase transitions,[7] being, essentially, phase transitions of the second kind. It is interesting to note that, according to the theoretically calculated[8] minima of the total energy, realization of a shape phase transition, from $\text{sign}\,\beta_2 > 0$ to $\text{sign}\,\beta_2 < 0$, requires the overcoming of only a very low (compared with the total energy) barrier with a height of about 0.5 MeV for intermediate nuclei. In view of the fact that the calculated quantities depend strongly on the choice of the free theoretical parameters, the especial importance of experiments and systematic data establishing the facts of shape phase transitions of nuclei becomes clear.

2. NUCLEAR-REACTION METHODS FOR OBTAINING THE ABSOLUTE MAGNITUDES AND SIGNS OF THE NUCLEAR DEFORMATION

Thus, from experimental data on elastic and inelastic scattering of nuclear particles by nuclei it is necessary to extract the following structure parameters: the nuclear radius R, the thickness ΔR of its surface layer, the nuclear matrix element $|C_1(2)|$ of the collective quadrupole transition to the first 2^+ state, the absolute magnitude of the nuclear quadrupole deformation parameter, $|\beta_2|$, and $\text{sign}\,\beta_2$, the sign of the nuclear quadrupole deformation parameter. From the experimental data of nuclear spectroscopy on the energies of the first 2^+ state for isotopic chains, it is necessary, after conversion in the framework of the superfluid model and normalization to the data on nuclear scattering, to obtain the absolute magnitudes $|\beta_2|$ of the nuclear quadrupole deformation; then, making a comparison with the results of theoretical calculations of sign β_2, data on the signs of the electric quadrupole moments, $\text{sign}\,Q_2$, and data on $\text{sign}\,\beta_2$ from inelastic nuclear scattering, it is necessary to recover $\text{sign}\,\beta_2$ for all isotopic chains and thereby create the entire surface with $\text{sign}\,\beta_2(Z,N)$ for all currently known nuclei.

Unfortunately, the practical realization of this mutual consistency problem is impossible in the framework of a single nuclear model, and one cannot avoid being eclectic in the analysis of the experimental data. However, this shortcoming is objectively transformed, given the volume of work and the number of nuclear parameters that are extracted, into the opposite. The advantage of such a global approach, in which one must mix different nuclear models in the analysis of the experimental data, is a certain model independence of the resulting nuclear-structure parameters, which are brought maximally close to the truth.

Choice of the reaction, species of bombarding particles, and the energy and angle ranges

A review of the types of nuclear reaction and of the methods used to obtain, from the angular distributions of the differential cross sections, the nuclear matrix elements $|C_1(2)|$, and then β_2, is given in our paper of Ref. 9. Since an analytic theory containing the sign of the nuclear deformation, $\text{sign}\,\beta_2$, as a parameter of the theory which can be unambiguously deduced from experiment has been developed only for elastic and inelastic scattering of α particles,[10] the choice of both the type of reaction and the species of particle is uniquely fixed (diffraction scattering of α particles).

The choice of the energy range E_α for the incident α particles is dictated by the requirement of the model of strong absorption, namely, the nucleus is "black" if

$$kR \gg 1, \tag{3}$$

where k is the wave number of the incident α particle. This means that the required range of energies is

$$E_\alpha = 15\text{–}150 \text{ MeV}. \tag{4}$$

The choice of the range of angles for measurement of the angular distributions of the differential cross sections of elastically and inelastically scattered α particles is more complicated and uncertain. Theoretical criteria arise here too from the requirements of strong absorption and are analogous to (3):

$$kR\theta \gg 1, \tag{5}$$

where θ is the scattering angle of the detected α particle. However, the condition (5) does not take into account

Coulomb effects and does not contain upper bounds. To establish a range of angles guaranteeing reliability, accuracy, and uniformity of the extracted nuclear parameters (i.e., their "purity" as regards the absence of nondiffraction scattering mechanisms and, therefore, renormalizations of their values), we made an empirical choice based on high statistics of the sample of angular distributions of differential cross sections:

$$(\theta_c \sim 15\text{–}20^\circ) \leqslant \theta \leqslant 75^\circ, \tag{6}$$

where θ_c is the Coulomb angle. The range (6) includes the fourth, fifth, sixth, and seventh Fraunhofer diffraction fringes, since the first, second, and third are strongly distorted by the Rutherford cross section and are not suitable for analysis, while at angles greater than 75° there come into play other, nondiffraction scattering mechanisms, and the number of free theoretical parameters must be increased in order to take them into account.

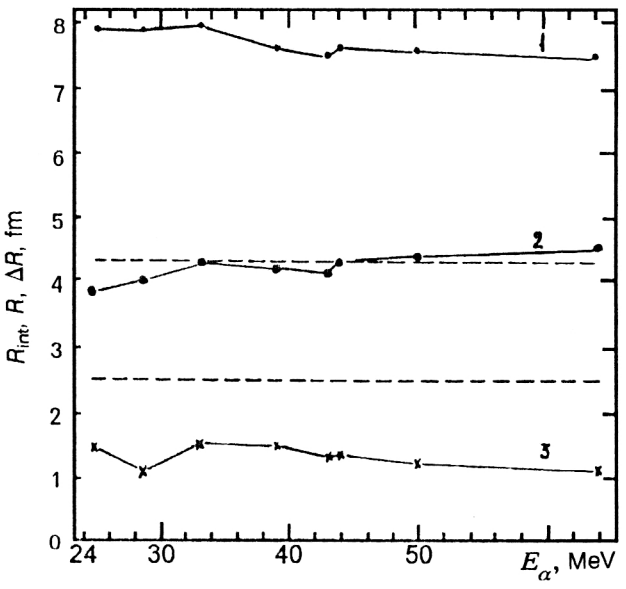

FIG. 1. Model dependence of radial structure parameters R_{int} (*1*), R (*2*), and ΔR (*3*) on the energy of the incident α particles. The broken lines show the values of R and ΔR obtained from electron scattering.[14]

Extraction from the experimental angular distributions of the differential cross sections of the nuclear radii *R* and the thicknesses Δ*R* of the nuclear surface layer

To extract $|\beta_2|$ from an experiment, it is necessary to know, as will be shown below, the nuclear radii R. Therefore, we consider the choice of the optimum method for obtaining the nuclear radii R and the thickness ΔR of the surface layer from elastic scattering of α particles having energies in the range (4). Thus, the extracted values must have the best accuracy and must be maximally free of model approximations and limitations. This task is also worthwhile because R and ΔR are also of great independent interest.

The nuclear radius R can be found from the semiclassical relation between the interaction range R_{int} and the orbital angular momentum l_0 for the trajectory of an incident particle that grazes the nuclear surface:[11]

$$R_{\text{int}} = \frac{1}{k}\left[n + \sqrt{n^2 + l_0(l_0+1)}\right], \tag{7}$$

where n is the Coulomb parameter (Sommerfeld parameter). It is usually recommended that the radius R of the nucleus itself should be found by subtracting the α-particle radius R_α and the range r_{NN} of the nuclear forces:[12]

$$R = R_{\text{int}} - R_\alpha - r_{NN}. \tag{8}$$

For $R_\alpha = 1.6$ fm, $r_{NN} = 1.0$ fm, Eq. (8) was particularized in Ref. 14 to

$$R = R_{\text{int}} - 2.6 \text{ fm}. \tag{9}$$

However, numerous measurements have shown[13] that the interaction range depends on the energy E_α (Fig. 1). To eliminate the energy dependence and obtain correctly the radius R of the nucleus itself from α-particle scattering, we introduce the more rigorous formula

$$R = R_{\text{int}} - \lambda\!\!\!^{-}_\alpha - r_{NN}, \tag{10}$$

where $\lambda\!\!\!^{-}_\alpha = 2\pi\lambda\!\!\!^{-}$ is the de Broglie wavelength of the α particle, which contains the energy dependence of R_{int}. It can be seen from Fig. 1 that the procedure (10) does indeed give the value of R as a universal constant. At the same time, the data on the nuclear radii R obtained from α-particle scattering agree satisfactorily with the data on electron scattering (Fig. 1). In principle, the thickness parameter ΔR of the surface layer should not exhibit an energy dependence, since for the incident α particle the boundary of the surface layer is weakly smeared.[14] This is also confirmed by Fig. 1. In absolute magnitude, the thickness ΔR, in contrast to R, differs appreciably from the value obtained in electron scattering (Fig. 1); the reason may be sought in the different radial distributions of the proton and neutron components in the nucleus.

The grazing angular momentum l_0, in its turn, is determined by computer fitting of the theoretical diffraction angular distribution of the differential cross section to the experimental cross section, and it is then used in the expression (7). The only rigorous formula for the scattering amplitude in quantum mechanics is the expression for the amplitude in the form of an expansion in partial waves:[15]

$$f(\theta) = \frac{1}{2ik}\sum_{l=0}^{\infty}(2l+1)\exp(2i\sigma_l)(S_l - 1)P_l(\cos\theta), \tag{11}$$

where all the notation is standard. The divergence of the sum over l in (11) due to $P_l(\cos\theta)$ can be eliminated by a special choice of the form of the S matrix with a cutoff of the fraction of the amplitude with large angular momenta. A practically felicitous parametrization, which makes it possible to implement this idea and does not distort the physical essence of the elastic interaction in this range in l, is the parametrization proposed in Ref. 16:

TABLE I. Optimum parameters of the model of parametrized phase-shift analysis obtained by fitting to experimental data.

Nucleus	E_α, MeV	l_1	l_2	λ_1	λ_2	b	R_1, fm	R_2, fm	ΔR_1, fm	ΔR_2, fm	σ_r, mb	σ_τ, mb
^{4}He	53.4	5.807	6.850	0.526	0.671	0.372	4.042	4.696	1.449	1.481	538.1	1002
^{6}Li	23.8	5.415	6.883	1.231	0.736	0.305	4.915	6.062	4.226	2.025	994.6	1533
^{7}Li	42	7.308	5.700	1.268	0.990	0.316	4.483	3.590	3.089	1.936	799.7	1280
^{9}Be	23.8	8.157	8.352	0.457	0.603	0.565	6.209	6.341	1.358	1.448	1072	2179
^{11}B	28.3	7.903	11.775	1.871	1.690	0.543	5.274	7.541	4.809	3.484	873.9	1772
^{12}C	29.3	8.90(3)	9.08(35)	0.50(2)	0.34(7)	0.349(4)	5.72(1)	5.83(20)	1.25(5)	0.67(13)	969.0	1796
	38.1	10.270	11.379	0.977	0.743	0.590	5.623	6.170	2.117	1.291	948.8	1826
	39.0	10.34(18)	10.4(2)	0.56(4)	0.53(9)	0.63(5)	5.56(8)	5.57(3)	1.16(8)	0.91(17)	874.5	1754
	40.4	10.52(1)	10.53(2)	0.55(1)	0.55(2)	0.47(10)	5.57(1)	5.58(1)	1.16(1)	0.93(3)	920.6	1769
	45.0	11.07(6)	11.01(4)	0.56(2)	0.62(6)	0.62(2)	5.48(3)	5.46(2)	1.12(3)	0.98(10)	854.9	1731
	50.5	11.68(1)	11.52(1)	0.57(1)	0.68(2)	0.503(1)	5.45(1)	5.38(1)	1.08(1)	1.03(3)	880.1	1727
^{13}C	28.4	8.328	11.058	0.151	0.104	0.609	5.637	6.887	0.371	0.205	-	-
^{14}N	37.9	10.808	13.666	0.812	1.599	0.385	5.745	7.109	1.700	2.686	934.8	1863
^{16}O	27.3	9.347	11.424	0.622	1.088	0.207	5.931	7.063	1.249	2.989	988.7	1840
	28.5	9.378	11.692	0.583	0.934	0.204	5.809	7.044	1.377	1.756	970.2	1777
	40.1	11.79(2)	11.89(3)	0.61(5)	0.61(3)	0.347(2)	5.38(9)	5.92(13)	1.20(10)	0.96(46)	1028	1928
	42	12.217	12.908	0.734	0.122	1.061	5.955	6.260	1.419	0.289	-	-
^{19}F	37.9	12.145	15.185	0.605	0.596	0.257	6.108	7.472	1.191	0.800	1102	2046
^{20}Ne	27.3	10.677	12.264	0.760	1.342	0.229	6.528	7.358	1.743	2.471	1204	2197
	28.5	10.594	12.155	0.712	1.333	0.196	6.333	7.131	1.599	2.402	1138	2070
	42	13.21	11.09	0.770	0.652	0.316	6.225	5.329	1.428	0.969	1165	2138
	104	20.396	20.708	1.322	0.659	0.467	5.787	5.871	1.561	0.624	1094	2011
^{24}Mg	22.5	9.836	10.368	0.253	0.192	0.264	6.768	7.065	0.618	0.376	-	-
	28.4	10.937	12.469	0.568	0.933	0.156	6.471	7.233	1.239	1.635	1128	2076
	39.0	13.27(1)	13.52(1)	0.68(1)	0.68(1)	0.352(1)	6.38(1)	6.49(1)	1.27(1)	1.01(1)	1153	2165
	42	13.888	17.155	0.707	0.145	0.242	6.416	7.757	1.274	0.210	-	-
	44	13.992	16.175	0.830	1.106	0.289	6.299	7.174	1.461	1.562	1159	2156
	50.5	15.13(5)	15.19(3)	0.72(14)	0.86(8)	0.349(1)	6.24(19)	6.26(118)	1.18(23)	1.13(131)	1137	2154
^{25}Mg	44	14.579	14.990	0.606	0.611	0.520	6.497	6.661	1.061	0.858	1125	2296
^{26}Mg	44	14.625	15.322	0.670	0.483	0.573	6.480	6.757	1.167	0.675	1179	2288
^{27}Al	40	13.729	13.850	0.405	0.125	0.732	6.462	6.512	0.735	0.182	-	-
^{28}Si	28.3	11.391	12.551	0.573	0.848	0.188	6.704	7.269	1.224	1.455	1167	2159
	39.0	13.85(1)	14.16(1)	0.71(1)	0.71(1)	0.349(1)	6.58(1)	6.71(1)	1.29(1)	1.04(2)	1202	2256
	50.5	15.85(3)	15.97(2)	0.75(5)	0.90(2)	0.349(1)	6.44(1)	6.49(6)	1.20(7)	1.16(30)	1192	2259
^{31}P	28.3	11.911	12.825	0.924	1.398	0.336	6.939	7.378	1.949	2.368	1247	2320
^{40}Ca	44	16.643	18.407	0.688	1.077	0.324	7.255	7.920	1.138	1.430	1389	2668
^{44}Ca	42	16.80	17.16	0.847	1.045	0.419	7.443	7.581	1.422	1.407	1459	2806
^{48}Ca	42	16.79	17.09	0.805	0.672	0.363	7.388	7.502	1.342	0.899	1471	2762
^{46}Ti	44	17.213	18.665	0.939	0.977	0.342	7.460	8.001	1.534	1.281	1491	2792
^{48}Ti	41	16.54	16.75	0.727	0.757	0.374	7.477	7.557	1.225	1.023	1443	2745
	44	16.725	19.265	1.859	1.045	0.412	7.254	8.197	3.026	1.366	1548	2698
^{50}Ti	44	17.278	18.763	0.926	0.972	0.355	7.436	7.986	1.503	1.266	1476	2776
^{52}Cr	29.0	13.22(4)	13.94(1)	0.76(2)	0.58(7)	0.318(1)	7.64(2)	7.96(5)	1.49(5)	0.91(11)	1341	2469
	40.4	16.30(1)	16.89(1)	0.83(1)	0.86(1)	0.350(1)	7.49(1)	7.72(1)	1.40(1)	1.17(1)	1425	2678
	44	17.267	18.782	0.960	0.833	0.427	7.490	8.049	1.552	1.081	1459	2753
	50.0	18.54(1)	18.99(1)	0.88(2)	1.05(7)	0.349(1)	7.37(1)	7.53(2)	1.32(3)	1.27(8)	1451	2750
^{54}Cr	38.0	16.260	16.458	0.798	0.738	0.378	7.720	7.798	1.381	1.024	1496	2821
^{54}Fe	16.53	8.784	9.682	0.402	0.0396	0.250	8.536	9.037	0.979	0.078	-	-
	29.3	13.22(3)	13.95(6)	0.77(2)	0.59(5)	0.353(3)	7.70(12)	8.02(29)	1.49(44)	0.93(70)	1314	2430
	38.0	15.993	17.034	0.940	0.871	0.361	7.708	8.118	1.623	1.208	1472	2741
	44	17.172	18.475	0.757	1.001	0.367	7.515	7.993	1.219	1.294	1409	2705
^{56}Fe	29.3	13.30(2)	14.06(5)	0.78(2)	0.59(3)	0.327(1)	7.77(10)	8.10(23)	1.51(46)	0.92(46)	1322	2473
	41	16.80	17.69	0.841	1.369	0.254	7.664	8.001	1.397	1.824	1481	2773
	44	17.738	18.841	0.954	1.200	0.360	7.704	8.108	1.533	1.547	1518	2875
^{58}Fe	21	10.647	11.243	0.682	0.447	0.219	8.141	8.445	1.522	0.803	1248	2248
	44	18.056	19.743	1.598	0.895	0.359	7.802	8.419	2.562	1.152	1704	3008
	45.0	17.92(3)	18.51(17)	0.88(5)	0.99(18)	0.307(77)	7.62(1)	7.82(6)	1.39(8)	1.25(23)	1504	2819
	50.5	19.15(3)	19.65(2)	0.90(2)	1.08(7)	0.349(3)	7.55(1)	7.72(2)	1.34(3)	1.30(8)	1505	2855
	64	22.17	22.28	0.979	1.09	0.341	7.576	7.609	1.308	1.167	1601	3031
^{58}Ni	24.7	11.437	12.310	0.777	0.426	0.245	7.862	8.275	1.609	0.711	-	-
	28.5	13.121	13.542	0.595	0.856	0.285	7.923	8.110	1.163	1.343	1302	2458
	33	14.95	15.41	0.87	0.51	0.41	7.96	8.15	1.58	0.74	1466	-
	40	15.94	16.85	0.991	0.808	0.371	7.516	7.863	1.658	1.085	1387	2566
	43	16.65	17.60	0.834	0.978	0.332	7.468	7.818	1.348	1.269	1373	2586
	44.4	17.85	17.31	0.897	0.391	0.524	7.766	7.570	1.430	0.499	1532	2868
	50.2	18.84	19.19	0.845	0.792	0.401	7.581	7.700	1.269	0.954	1479	2813

TABLE I. (*Continued.*)

Nucleus	E_α, MeV	l_1	l_2	λ_1	λ_2	b	R_1, fm	R_2, fm	ΔR_1, fm	ΔR_2, fm	σ_τ, mb	σ_τ, mb
^{58}Ni	50.5	18.95(4)	19.45(11)	0.90(3)	1.09(13)	0.339(6)	7.55(1)	7.72(4)	1.34(5)	1.30(14)	1479	2798
	64.3	21.80	21.90	0.861	0.991	0.380	7.496	7.527	1.146	1.058	1520	2916
^{60}Ni	38.0	15.959	16.723	1.037	0.822	0.308	7.736	8.034	1.775	1.129	1482	2698
	43	18.304	18.960	1.101	0.628	0.625	8.060	8.302	1.780	0.814	1622	3107
	44	17.890	19.150	1.183	0.778	0.319	7.804	8.263	1.890	0.998	1605	2911
^{62}Ni	38.0	16.153	16.980	1.066	0.781	0.273	7.796	8.118	1.821	1.071	1523	2752
	43	13.039	12.216	1.080	1.118	0.949	6.117	5.817	1.727	1.430	640.9	1620
	44	18.536	18.692	0.933	0.837	0.376	8.023	8.080	1.488	1.071	1643	3088
	50.5	19.27(2)	19.82(14)	0.91(4)	1.09(14)	0.327(6)	7.67(1)	7.86(5)	1.36(6)	1.31(16)	1536	2899
^{64}Ni	21.3	10.332	11.439	0.849	0.166	0.471	8.049	8.602	1.851	0.293	-	-
	40	16.31	17.19	0.891	0.856	0.222	7.611	7.945	1.482	1.143	1442	2643
^{63}Cu	44	18.805	19.634	1.073	1.547	0.335	8.153	8.454	1.709	1.978	1685	3177
^{65}Cu	44	18.924	19.686	0.999	1.290	0.299	8.181	8.457	1.589	1.646	1711	3200
^{64}Zn	29.0	13.38(1)	14.21(1)	0.80(3)	0.62(2)	0.251(2)	7.99(1)	8.36(1)	1.53(5)	0.95(3)	1323	2463
	38.0	16.25(1)	16.98(1)	0.86(1)	0.87(1)	0.267(1)	7.87(1)	8.16(1)	1.46(1)	1.18(1)	1477	2730
	40	16.48	17.86	0.912	0.928	0.282	7.765	8.288	1.515	1.238	1459	2697
	41	17.254	18.025	1.006	1.004	0.274	7.943	8.232	1.653	1.324	1568	2880
	43	17.636	18.386	0.990	0.931	0.283	7.866	8.140	1.590	1.200	1564	2863
	44	18.032	18.456	0.977	1.135	0.274	7.905	8.059	1.553	1.447	1576	2920
	50.5	19.39(3)	19.95(11)	0.92(4)	1.11(13)	0.350(1)	7.72(1)	7.91(4)	1.36(6)	1.32(15)	1525	2891
^{66}Zn	29.0	13.54(5)	14.38(3)	0.81(4)	0.63(8)	0.256(1)	8.05(2)	8.42(1)	1.64(8)	0.96(11)	1378	2511
	38.0	16.43(1)	17.18(1)	0.87(1)	0.875(1)	0.36(1)	7.93(1)	8.22(1)	1.47(1)	1.19(1)	1482	2778
	50.5	19.47(4)	20.05(8)	0.92(4)	1.11(1)	0.384(5)	7.78(1)	7.97(3)	1.37(6)	1.32(12)	1539	2940
^{68}Zn	29.0	13.70(5)	14.55(2)	0.81(3)	0.63(6)	0.225(1)	8.11(2)	8.48(1)	1.55(6)	0.97(10)	1407	2557
	38.0	16.60(1)	17.37(1)	0.87(1)	0.88(1)	0.249(1)	7.98(1)	8.28(1)	1.48(1)	1.19(1)	1531	2826
	40	16.66	17.47	1.025	0.808	0.242	7.806	8.112	1.697	1.074	1512	2742
	43	17.90	18.67	1.017	0.787	0.266	-	-	-	-	-	-
	50.5	19.79(2)	20.39(4)	0.93(2)	1.13(5)	0.300(8)	7.83(1)	8.03(1)	1.38(2)	1.33(6)	1585	2988
^{70}Zn	29.0	13.85(6)	14.72(3)	0.82(3)	0.64(8)	0.229(1)	8.16(2)	8.54(1)	1.56(7)	0.97(12)	1434	2603
	38.0	16.77(1)	17.56(1)	0.88(1)	0.89(1)	0.319(1)	8.03(1)	8.34(1)	1.48(1)	1.20(1)	1540	2873
	50.5	19.99(4)	20.60(1)	0.94(5)	1.13(10)	0.347(1)	7.88(1)	8.09(4)	1.38(7)	1.34(12)	1601	3036
^{74}Ge	39.0	17.53	19.38	0.99	1.23	0.26	8.26	8.96	1.65	1.63	1641	
^{84}Kr	38.4	18.60	17.84	0.976	0.504	0.266	8.926	8.638	1.627	0.673	1885	3453
^{88}Sr	42	18.66	18.81	0.868	0.681	0.311	8.554	8.609	1.380	0.868	1692	3157
^{89}Y	42	18.777	18.887	0.811	0.813	0.366	8.635	8.675	1.288	1.035	1681	3190
^{90}Zr	50.1	20.98(3)	21.60(7)	0.99(5)	1.10(11)	0.366(11)	8.54(1)	8.75(2)	1.45(6)	1.29(10)	1751	3322
^{92}Zr	65	27.32	28.80	1.80	1.70	0.250	9.205	9.640	2.323	1.761	2387	4315
^{94}Zr	50.1	21.47(3)	22.12(6)	1.12(4)	0.99(10)	0.305(7)	8.69(1)	8.90(2)	1.63(6)	1.16(12)	1868	3466
^{92}Mo	31	14.854	15.423	0.682	0.742	0.339	8.917	9.150	1.226	1.073	1447	2737
	38.0	17.031	17.633	0.927	0.546	0.301	8.641	8.868	1.530	0.724	1590	2918
	49.2	21.36(5)	22.11(6)	1.30(5)	0.99(10)	0.210(8)	8.82(2)	9.07(2)	1.91(7)	1.16(12)	1944	3513
^{94}Mo	50.5	21.46(11)	22.35(16)	0.99(12)	1.12(32)	0.361(32)	8.71(3)	9.01(6)	1.44(18)	1.30(37)	1805	3429
^{96}Mo	45.0	19.90(8)	20.76(14)	0.82(10)	1.31(32)	0.405(35)	8.77(3)	9.07(5)	1.29(16)	1.60(39)	1692	3311
^{98}Mo	40	17.443	18.392	1.079	0.222	0.172	8.501	8.849	1.736	0.287		
	45.0	20.37(7)	21.20(12)	1.07(9)	1.15(19)	0.333(17)	8.93(2)	9.22(4)	1.64(14)	1.41(24)	1855	3472
^{100}Mo	38.0	17.407	18.06	1.109	0.743	0.139	8.753	8.998	1.826	0.983	1696	3035
^{106}Pd	38.0	17.59	18.37	1.03	1.12	0.205	8.998	9.289	1.685	1.472	1690	3078
^{107}Ag	40	17.07	20.54	1.969	1.069	0.151	8.569	9.834	3.133	1.377	1713	2840
^{112}Sn	44	20.37	20.98	0.907	1.56	0.440	9.331	9.544	1.386	1.914	1767	3508
	50.1	21.26(11)	22.62(7)	1.40(11)	0.88(11)	0.325(16)	8.92(3)	9.36(2)	2.01(15)	1.02(12)	1862	3375
^{114}Sn	44	20.51	21.02	0.883	1.66	0.413	9.374	9.552	1.349	2.036	1793	3550
	50.1	21.68(12)	23.03(10)	1.71(13)	0.95(15)	0.290(20)	9.05(4)	9.49(3)	2.45(19)	1.09(17)	1992	3522
^{116}Sn	40.4	17.96(28)	19.87(16)	1.43(18)	0.76(24)	0.315(45)	8.95(10)	9.64(6)	2.25(29)	0.97(31)	1705	3023
	44	20.010	20.54	1.032	1.443	0.366	9.195	9.379	1.574	1.767	1776	3387
	65.7	26.42	26.80	1.11	1.45	0.280	9.067	9.176	1.407	1.474	2064	3897
^{118}Sn	44	19.486	19.839	0.964	1.43	0.354	9.008	9.130	1.467	1.747	1681	3211
^{120}Sn	44	19.343	19.613	1.108	1.49	0.288	8.953	9.047	1.685	1.818	1707	3169
	50.5	22.17(6)	22.8(1)	1.04(6)	1.27(15)	0.322(14)	9.15(2)	9.34(4)	1.48(9)	1.46(18)	1902	3502
^{122}Sn	44	19.889	20.153	1.084	1.289	0.300	9.138	9.229	1.650	1.574	1795	3340
^{124}Sn	40.4	18.9(4)	20.8(4)	1.41(25)	1.08(51)	0.24(6)	9.26(14)	9.96(14)	2.23(38)	1.37(65)	1860	3308
	50.5	22.36(5)	22.8(2)	1.04(5)	1.29(3)	0.298(13)	9.20(2)	9.33(7)	1.49(7)	1.48(15)	1939	3646
^{122}Te	42	19.056	19.339	0.961	1.008	0.257	9.196	9.296	1.488	1.253	1734	3214
^{124}Te	42	18.717	18.872	0.944	1.082	0.249	9.072	9.127	1.460	1.342	1673	3101
^{126}Te	42	19.517	19.807	0.986	1.087	0.254	9.349	9.452	1.528	1.351	1813	3361
^{128}Te	42	19.335	19.720	0.992	1.051	0.251	9.281	9.417	1.535	1.306	1783	3298
^{130}Te	42	19.474	19.777	0.990	1.078	0.261	9.325	9.432	1.532	1.339	1801	3341

TABLE I. (*Continued.*)

Nucleus	E_α, MeV	l_1	l_2	λ_1	λ_2	b	R_1, fm	R_2, fm	ΔR_1, fm	ΔR_2, fm	σ_r, mb	σ_τ, mb
^{148}Sm	50	23.300	23.172	1.180	1.202	0.246	9.943	9.902	1.676	1.368	2140	3955
^{150}Sm	50	22.706	23.097	1.120	1.376	0.278	9.748	9.874	1.588	1.565	2011	3756
^{152}Sm	50	22.777	22.966	1.208	1.379	0.281	9.767	9.838	1.712	1.568	2038	3781
^{166}Er	50	24.789	24.018	1.474	1.608	0.144	10.612	10.364	2.084	1.819	2468	4453
^{176}Yb	50	23.278	23.225	1.257	1.408	0.243	10.186	10.169	1.765	1.585	2129	3919
^{206}Pb	39.0	17.47	17.97	1.24	3.36	0.47	10.42	-	1.84	-	-	-
^{207}Pb	39.0	17.07	19.41	1.42	1.09	0.38	10.28	-	2.09	-	-	-
^{208}Pb	39.0	17.71	18.99	0.92	0.86	0.34	10.50	10.93	1.36	1.03	1490	-

Notes:

1) Data on the optimum parameters of the parametrized phase-shift analysis are taken in part from Refs. 19 and 21–24; most were obtained by the author.

2) For references to the literature sources, see Ref. 20.

3) The errors in the parameters of the parametrized phase-shift analysis and other quantities given in brackets were obtained either by averaging from series of fits or on the basis of the errors of the original experimental data.

4) The parameters R_1 and R_2 were calculated in accordance with Eq. (7), ΔR_1 and ΔR_2 in accordance with (13), and σ_r and σ_τ were calculated in accordance with the formulas in Ref. 15.

$$S_l = U + iV,$$

$$U = \left[1+\exp\left(\frac{l_1-l}{\lambda_1}\right)\right]^{-1}, \quad V = b\cosh^{-2}\left(\frac{l-l_2}{2\lambda_2}\right), \quad (12)$$

where the real part of the S matrix is parametrized in the form of a smeared Fermi step, and the imaginary part in the form of a bell-shaped function localized on the nuclear surface; l_1, l_2, λ_1, λ_2, b are five free parameters of the theory, of which we identify the parameter l_1 with the angular momentum l_0, while the smearing ΔR of the nuclear edge is determined from the parameter λ_1 (corresponding formulas and the text of a FORTRAN program can be found in Ref. 17). It can be seen from (12) that the shape of the real part of the S matrix (in the form of a smeared Fermi step) matches the shape of the radial distribution of the nuclear density,[14,18] and, therefore, this parametrization of the S matrix is adequate and satisfies the necessary requirements for the practical extraction of the nuclear radius by comparing the theoretical [(11) and (12)] with the experimental angular distributions of the differential cross sections.

The analytical realizations of the theoretical angular distributions of the differential cross sections from (11), for example, in Ref. 12, in the sense of extraction of the radial parameters R and ΔR do not satisfy the practical requirements of accuracy[19] and deviate systematically from the values obtained in the framework of the exact parametrized phase-shift analysis (11)–(12) made above. The value of ΔR in this analysis is

$$\Delta R = \frac{2.2(2l_1+1)\lambda_1}{k\sqrt{n^2+l_1(l_1+1)}}. \quad (13)$$

Table I gives systematized[20] data on the optimal parameters of the analysis from Eqs. (11) and (12) obtained by fitting the theory to the experimental data. Table II contains data on the nuclear radii R and the thicknesses ΔR of the surface layer obtained from the interaction ranges $R_{\text{int}} = R_1$ in accordance with the procedure (10), which therefore do not depend on the α-particle energy; in brackets, we give for comparison individual data on electron scattering.[14] For the nuclei for which in the world literature there were experimental data on the angular distributions of the differential cross sections for different α-particle energies, we formed, after the procedure (10), a sample (by rejecting the least and greatest values) with subsequent averaging and calculation of the rms errors. Table III gives the optimum parameters of the model of the method of complex angular momenta, and also the de Broglie wavelength parameters $\lambda\!\!\!^{-} = 1/k$. The completeness and systematization of the values given in Table II enable us to hope that the data on R and ΔR in it are the most accurate of all known data in the literature obtained from α-particle scattering.

We should like to emphasize once more that the values of R and ΔR, obtained, not from the rigorous formula (11), but from analytic realizations of it of the type in Ref. 12, are not suitable for comparisons with data on electron scattering, μ-mesic atoms, proton scattering, and other independent methods because of the uncontrollable approximations made in analytic models and the systematic deformations from rigorous theory, for which in the given case we have the expansion (11) of the scattering amplitude with respect to partial waves.

Extraction of the absolute values of the nuclear quadrupole deformation parameters from the angular distributions of the differential cross sections

The parameter $|\beta_2|$ is related to the nuclear matrix element $|C_1(2)|$ by[10,12,16]

$$|\beta_2| = \frac{2.24|C_1(2)|}{l_0/k-2.6}. \quad (14)$$

TABLE II. Nuclear radii R and thickness ΔR of the surface layer obtained from α-particle scattering.

Nucleus	Radius of nucleus R, fm		Thickness of surface layer ΔR, fm		Nucleus	Radius of nucleus R, fm		Thickness of surface layer ΔR, fm	
^{4}He	1.02	(1.10)	1.45	(1.4)	^{58}Ni	4.27	(4.28)	1.44	(2.5)
^{6}Li	1.46	(1.56)	4.23	(2.3)	^{60}Ni	4.51		1.78	
^{7}Li	1.24		3.09		^{62}Ni	4.53		1.52	
^{9}Be	0.981	(1.80)	1.36	(2.0)	^{64}Ni	4.21		1.48	
^{11}B	0.614	(2.00)	4.81	(2.0)	^{63}Cu	4.86		1.71	
^{12}C	1.56	(2.30)	1.17	(1.85)	^{65}Cu	4.90		1.59	
^{13}C	1.13		0.371		^{64}Zn	4.52		1.66	
^{14}N	1.76	(2.40)	1.70	(1.85)	^{66}Zn	4.45		1.49	
^{16}O	1.52	(2.60)	1.28	(1.8)	^{68}Zn	4.49		1.53	
^{19}F	2.30		1.19		^{70}Zn	4.57		1.47	
^{20}Ne	2.32		1.58		^{74}Ge	4.85		1.65	
^{24}Mg	2.67	(2.93)	1.26	(2.6)	^{84}Kr	5.51		1.63	
^{25}Mg	3.0		1.06		^{88}Sr	5.25	(4.80)	1.38	(2.3)
^{26}Mg	3.0		1.17		^{89}Y	5.33		1.29	
^{27}Al	2.87		0.735		^{90}Zr	5.43		1.45	
^{28}Si	2.92	(2.95)	1.24	(2.8)	^{92}Zr	6.36		2.32	
^{31}P	2.91		1.95		^{94}Zr	5.59		1.63	
^{32}S	-	(3.26)	-	(2.6)	^{92}Mo	5.39		1.55	
^{40}Ca	3.89	(3.64)	1.14	(2.5)	^{94}Mo	5.62		1.44	
^{44}Ca	4.04		1.42		^{96}Mo	5.55		1.29	
^{48}Ca	4.00		1.34		^{98}Mo	5.43		1.69	
^{46}Ti	4.12		1.53		^{100}Mo	5.34		1.83	
^{48}Ti	3.99		1.23		^{106}Pd	5.59		1.69	
^{50}Ti	4.11		1.50		^{107}Ag	5.23		3.13	
^{51}V	-	(3.98)	-	(2.2)	^{115}In	-	(5.24)	-	(2.3)
^{52}Cr	4.06		1.44		^{112}Sn	5.96		1.70	
^{54}Cr	4.23		1.38		^{114}Sn	6.03		1.90	
^{54}Fe	4.09		1.45		^{116}Sn	5.95		1.75	
^{56}Fe	4.21		1.48		^{118}Sn	5.78		1.47	
^{58}Fe	4.48		1.35		^{120}Sn	5.90		1.59	
^{59}Co	-	(4.09)	-	(2.5)	^{122}Sn	5.92		1.65	
^{124}Sn	6.04		1.86		^{152}Sm	6.69		1.71	
^{122}Sb	-	(5.32)	-	(2.5)	^{166}Er	7.54		2.08	
^{122}Te	5.92		1.49		^{176}Yb	7.12		1.77	
^{124}Te	5.80		1.46		^{181}Ta	-	(6.45)	-	(2.8)
^{126}Te	6.08		1.53		^{197}Au	-	(6.38)	-	(2.32)
^{128}Te	6.01		1.54		^{206}Pb	7.09		1.84	
^{130}Te	6.05		1.53		^{207}Pb	6.95		2.09	
^{148}Sm	6.87		1.68		^{208}Pb	7.17	(6.5)	1.36	(2.3)
^{150}Sm	6.68		1.59		^{209}Bi	-	(6.47)	-	(2.7)

Notes:

[1)] The values of R and ΔR obtained from electron scattering[14] are given in brackets.

[2)] The errors in R and ΔR are 1–3 (rarely 5–6) units in the last significant figure.

[3)] The parameters of nuclei for which measurements at different energies of the incident α particles were made were obtained by estimating the reliability of the primary experimental data and subsequent averaging of the parameters R and ΔR for the different energies.

[4)] In the ^{4}He$(\alpha,\alpha)^{4}$He case of scattering of identical particles the operation for determining the radius was different in accordance with the physical meaning $R=R_{\text{int}}/2-r_{NN}$; the radii for ^{6}Li and ^{7}Li were found similarly in connection with the large contribution of the ^{4}He cluster component.

Rigorous expressions for the amplitudes of the inelastic interaction of α particles with nuclei, such as for the elastic interaction in the form (11), do not exist, but there are analytic realizations of the expression (11). The most internally consistent theory of inelastic scattering has been given by Inopin *et al.*[10,12,16] In the framework of this theory, the cross sections of elastic and inelastic (with excitation of collective states) scattering have the form

$$\sigma_0=\frac{8\pi}{k^2}\,|a|^2 l_0 \sin^{-1}\theta \exp(-2\beta\theta) \times\{b^2+\cos^2[(l_0+0.5)\theta+\gamma]\},$$

$$\sigma_I=2(2I+1)\,|a|^2|C_n(I)|^2 l_0\theta^2 \sin^{-1}\theta \exp(-2\beta\theta)\left\{b^2+\cos^2\left[\left(l_0+\frac{1}{2}\right)\theta+\gamma+\frac{\pi}{2}(I+1)\right]\right\}, \tag{15}$$

where l_0, $|\alpha|$, β, b, γ are five free parameters of the theory, and the remaining notation is standard. Leaving on one side the problem of obtaining the free parameters of the theory (the procedures can be found in Refs. 9, 13, and 25), we concentrate solely on the extraction from experiment of the nuclear matrix element $|C_1(2)|$. It was shown in Ref. 26, and in our studies of Refs. 9, 13, 19, and 25 we verified on numerous experimental data of our own as well as data given in the literature, that a correct and fairly rigorous expression for $|C_1(2)|$ is the following:

TABLE III. Optimum parameters of the model of the method of complex angular momenta.

Nucleus	E_α, MeV	k, fm^{-1}	θ_c, deg	l_0	β	b	$\lvert a\rvert$	γ	$\lvert C_1(2)\rvert$, fm	$\lvert\beta_2\rvert$
$^{12}_{6}$C	18	1.40	16.4	6.22(5)	0.29(1)	0.70(1)	0.53(1)	2.04(1)	0.59(1)	0.36(3)
	20.16	1.48	15.3	6.29(5)	0.59(1)	0.34(1)	0.72(1)	1.84(1)	0.58(1)	0.38(3)
	22.75	1.57	13.3	6.82(6)	0.60(1)	0.14(1)	1.07(2)	1.76(1)	0.84(1)	0.56(4)
	24	1.62	13.2	6.70(6)	1.28(1)	0.37(1)	3.32(5)	1.86(1)	0.59(1)	0.42(3)
	26.1	1.68	11.8	7.19(7)	1.57(2)	0.60(1)	2.18(4)	2.12(1)	0.75(1)	0.52(4)
	29.3	1.79	9.9	8.07(8)	2.16(2)	0.76(1)	4.1(1)	1.64(1)	0.48(1)	0.32(2)
	31.5	1.85	8.5	9.1(1)	1.63(2)	0.68(1)	2.42(5)	1.54(1)	0.65(1)	0.39(2)
	33.4	1.91	8.6	8.73(9)	2.20(3)	0.42(1)	4.2(1)	1.45(1)	0.50(1)	0.33(2)
	36	1.98	9.4	7.68(7)	1.86(2)	0.14(1)	3.68(7)	2.40(1)	0.46(1)	0.39(3)
	39.0	2.06	8.3	8.41(9)	0.88(3)	0.70(1)	0.80(3)	2.15(1)	0.64(1)	0.50(4)
	40.4	2.09	7.3	9.3(1)	2.20(3)	0.48(1)	2.68(8)	1.70(1)	0.69(1)	0.48(3)
	40.5	2.10	7.3	9.3(1)	2.42(3)	0.12(1)	3.8(1)	1.82(1)	0.73(1)	0.52(3)
	41	2.11	7.4	9.2(1)	2.27(3)	0.20(1)	3.25(8)	1.94(1)	0.71(1)	0.52(3)
	45.0	2.21	6.6	9.9(1)	0.57(2)	0.84(1)	0.64(2)	1.52(1)	0.57(1)	0.41(2)
	50.5	2.35	6.1	10.1(1)	1.80(3)	0.32(1)	2.41(6)	1.85(1)	0.52(1)	0.40(3)
	60	2.56	5.1	11.0(2)	1.54(3)	0.51(1)	1.80(4)	1.85(1)	0.52(1)	0.40(3)
	65	2.66	4.4	12.4(2)	2.51(5)	0.27(1)	2.14(7)	0.67(1)	0.33(1)	0.23(1)
	104	3.36	2.9	14.5(3)	2.86(6)	0.64(1)	3.0(1)	1.99(1)	0.60(1)	0.49(3)
	139	3.89	2.0	18.3(4)	3.10(9)	0.79(1)	2.8(1)	1.11(1)	0.48(1)	0.35(2)
	1370	12.21	0.36	32.8(2)	19.6(8)	0.26(1)	12(2)	2.09(1)	0.65(1)	1.55(29)
$^{16}_{8}$O	18.3	1.51	19.2	7.00(6)	0.13(1)	0.27(1)	1.22(1)	1.96(1)	0.29(1)	0.16(1)
	21.8	1.64	16.1	7.68(3)	2.12(3)	0.24(1)	3.0(2)	2.57(1)	0.60(1)	0.35(3)
	23.7	1.71	13.1	9.07(5)	0.67(1)	0.27(1)	1.23(2)	0.97(1)	0.34(1)	0.17(1)
	27.3	1.84	13.1	8.4(4)	1.40(9)	0.36(2)	1.7(2)	1.93(2)	0.46(3)	0.28(3)
	40.1	2.23	7.9	11.5(2)	2.0(1)	1.09(8)	2.2(5)	3.7(2)	0.24(3)	0.18(3)
	40.5	2.24	8.2	11.11(7)	3.21(3)	0.18(1)	4.69(8)	1.67(1)	0.36(1)	0.22(1)
	104	3.59	3.2	17.9(3)	4.75(6)	0.56(1)	5.3(2)	4.62(1)	0.35(1)	0.23(1)
$^{24}_{12}$Mg	12.7	1.34	36.7	6.4(3)	1.05(5)	0.10(1)	1.9(1)	1.45(2)	0.57(39)	0.25(19)
	31.5	2.12	13.9	11.11(7)	2.45(2)	0.30(1)	3.54(5)	1.42(2)	0.59(1)	0.30(2)
	39.0	2.35	10.9	12.7(3)	2.88(8)	0.31(1)	3.9(3)	4.5(1)	0.72(2)	0.46(5)
	42	2.44	10.5	12.7(1)	3.49(4)	0.10(1)	4.9(1)	1.75(1)	0.68(1)	0.37(2)
	50.5	2.68	7.6	16.1(5)	2.3(1)	0.51(2)	2.3(2)	3.5(2)	0.88(1)	0.50(4)
$^{28}_{14}$Si	16.2	1.55	33.4	7.3(3)	3.5(2)	0.97(1)	11(2)	2.18(2)	0.60(1)	0.27(4)
	19.5	1.70	27.9	8.1(4)	3.3(2)	0.83(2)	9(1)	2.09(2)	0.59(4)	0.29(2)
	21.6	1.79	24.2	8.9(5)	1.33(9)	0.59(2)	1.8(2)	1.57(2)	0.63(4)	0.31(4)
	23.3	1.86	23.3	8.9(5)	3.6(2)	0.39(1)	12(2)	1.57(2)	0.45(11)	0.23(7)
	25.1	1.93	25.9	7.7(4)	1.01(6)	0.13(4)	1.9(2)	0.43(2)	0.55(5)	0.36(6)
	27	2.00	19.2	10.09(6)	1.45(2)	0.35(1)	1.83(5)	1.66(2)	0.82(1)	0.42(4)
	39.0	2.40	13.7	11.8(3)	1.71(8)	0.44(3)	1.5(1)	2.4(2)	0.72(5)	0.45(8)
	41	2.46	12.8	12.4(9)	1.3(1)	0.78(1)	2.1(3)	2.24(2)	0.50(5)	0.10(1)
	50.5	2.74	9.2	15.5(4)	2.7(1)	0.39(2)	2.8(2)	4.3(2)	0.25(4)	0.15(3)
	104	3.93	4.8	21(3)	5.4(8)	0.29(1)	7(2)	1.57(2)	0.60(11)	0.34(8)
$^{48}_{22}$Ti	27.2	2.12	25.1	12.0(9)	5.0(4)	0.25(1)	17(6)	0.92(2)	0.45(5)	0.18(3)
	28.4	2.16	24.7	11.9(9)	2.5(2)	0.23(1)	3.7(8)	2.17(2)	0.40(3)	0.17(2)
	31	2.26	22.0	12.8(10)	2.9(3)	0.30(3)	4.4(9)	2.09(2)	0.59(9)	0.25(5)
	50.5	2.89	12.5	17.9(6)	3.3(1)	0.29(1)	3.9(5)	1.1(3)	0.29(5)	0.15(3)
	104	4.14	5.9	26.7(8)	4.8(2)	0.29(1)	4.8(4)	1.51(1)	0.43(2)	0.19(1)
	140	4.81	4.9	27.5(9)	7.4(3)	0.21(1)	10.2(8)	1.94(3)	0.37(5)	0.19(3)
$^{52}_{24}$Cr	29.0	2.20	25.1	12.7(3)	3.07(8)	0.46(1)	6.0(4)	1.54(14)	0.43(5)	0.20(5)
	40.4	2.60	14.9	18.3(4)	3.72(9)	0.16(1)	8.4(5)	3.08(1)	0.20(1)	0.07(1)
	50.0	2.90	13.9	17.5(5)	2.65(10)	0.25(1)	2.6(2)	1.41(24)	0.22(5)	0.11(3)
$^{54}_{26}$Fe	16.05	1.64	51.5	8.5(5)	2.64(15)	1.47(4)	7.8(18)	2.36(2)	0.22(1)	0.07(1)
	29.3	2.22	27.1	12.6(3)	3.92(10)	0.51(1)	12.4(11)	1.6(1)	0.21(3)	0.10(1)
$^{56}_{26}$Fe	29.3	2.22	24.1	14.2(4)	3.43(11)	0.64(1)	6.4(6)	3.8(2)	0.38(6)	0.16(4)
	104	4.19	7.3	25(4)	4.9(9)	0.195(1)	5.6(4)	2.24(2)	0.33(13)	0.16(7)
$^{58}_{26}$Fe	45.0	2.76	16.5	16.9(3)	3.57(9)	0.18(1)	5.6(4)	1.89(1)	0.39(10)	0.16(1)
	50.5	2.92	14.8	17.9(6)	3.3(6)	0.47(11)	4.1(2)	1.7(3)	0.36(8)	0.18(5)
	64.3	3.30	10.6	22(3)	4.4(6)	0.27(1)	7.7(6)	1.18(1)	0.25(1)	0.10(1)
$^{58}_{28}$Ni	32.3	2.34	31.3	11.1(8)	3.0(2)	0.27(1)	6.0(13)	3.65(8)	0.36(8)	0.17(5)
	34.4	2.41	25.5	13.4(11)	3.2(3)	0.48(2)	6.1(13)	2.66(2)	0.33(44)	0.14(21)
	42	2.67	26.0	11.8(8)	3.5(3)	0.84(1)	5.2(11)	0.90(2)	0.32(1)	0.10(4)
	43	2.70	18.4	16.6(16)	3.9(5)	0.40(1)	7.5(24)	1.05(2)	0.33(9)	0.13(4)
	50.2	2.92	15.4	18.5(4)	3.82(9)	0.10(1)	6.0(4)	1.65(2)	0.26(1)	0.104(10)
	50.5	2.93	16.2	17.5(5)	3.0(7)	0.38(13)	2.9(19)	1.9(3)	0.31(17)	0.15(1)
	64.3	3.30	12.3	20.4(5)	4.1(2)	0.26(1)	2.5(3)	1.97(2)	0.29(5)	0.12(2)
	152	5.07	6.5	25.2(7)	6.6(3)	0.37(1)	8.5(7)	2.92(1)	0.47(6)	0.30(3)
	1370	15.23	0.74	74.5(63)	28.6(26)	0.66(1)	15.3(74)	2.36(1)	0.58(1)	0.41(4)
$^{62}_{28}$Ni	32.3	2.35	26.1	13.5(11)	3.0(3)	0.41(1)	4.7(12)	2.48(2)	0.44(5)	0.17(3)
	33	2.37	25.0	13.9(11)	1.1(1)	0.42(1)	0.84(10)	1.57(2)	0.67(8)	0.26(15)

TABLE III. (*Continued.*)

Nucleus	E_α, MeV	k, fm^{-1}	θ_c, deg	l_0	β	b	$\lvert a\rvert$	γ	$\lvert C_1(2)\rvert$, fm	$\lvert\beta_2\rvert$
$^{62}_{28}$Ni	50	2.94	14.2	20.1(24)	3.3(5)	0.25(1)	6.0(17)	2.69(2)	0.33(7)	0.12(3)
	50.5	2.94	14.6	19.5(4)	3.9(1)	0.11(1)	6.0(5)	0.70(1)	0.42(1)	0.12(3)
	100	4.13	6.4	32(6)	7.4(15)	0.28(1)	14(9)	2.80(2)	0.44(8)	0.15(3)
$^{64}_{30}$Zn	22	1.95	50.4	9.20	1.79	0.45	0.82	0.56	0.24	0.110
	29.0	2.23	30.5	12.8(3)	2.7(6)	0.38(1)	4.6(36)	2.1(2)	0.31(20)	0.14(10)
	38.0	2.55	22.4	15.6(4)	3.2(2)	0.27(3)	4.7(10)	1.7(3)	0.32(15)	0.14(8)
	40	2.62	20.6	16.2	3.6	0.36	6.9	1.38	0.42	0.19
	43	2.72	20.1	16.3	4.3	0.38	9.8	2.11	0.48	0.23
	50.5	2.93	16.3	18.7(8)	3.96(20)	0.40(1)	5.8(9)	1.9(3)	0.27(6)	0.12(3)
$^{66}_{30}$Zn	29.0	2.23	29.4	13.4(3)	2.9(1)	0.39(1)	6.0(10)	1.7(2)	0.42(16)	0.18(9)
	38.0	2.56	22.2	15.7(4)	3.6(2)	0.23(1)	7.0(1)	1.9(3)	0.37(16)	0.17(8)
	43	2.72	19.2	17.1	4.0	0.54	6.9	1.77	0.34	0.149
	50.5	2.93	14.7	20.7(8)	3.8(2)	0.21(1)	4.9(9)	0.37(37)	0.35(1)	0.14(5)
$^{68}_{30}$Zn	29.0	2.24	30.3	12.9(3)	2.8(1)	0.44(1)	5.1(8)	2.3(2)	0.41(18)	0.18(10)
	38.0	2.56	21.5	16.7(5)	4.0(1)	0.35(1)	8.7(10)	1.1(2)	0.32(2)	0.13(3)
	40	2.63	20.4	15.7	3.52	0.36	6.08	2.10	0.46	0.23
	43	2.73	20.0	16.4	4.08	0.44	8.16	2.16	0.39	0.18
	50.5	2.94	17.7	17.2(4)	4.22(9)	0.24(1)	8.1(6)	3.08(1)	0.36(1)	0.12(5)
$^{70}_{30}$Zn	29.0	2.24	28.3	13.9(3)	3.98(11)	0.64(1)	14.0(2)	4.5(2)	0.45(1)	0.18(6)
	38.0	2.56	20.8	16.8(5)	3.48(12)	0.48(1)	5.2(6)	1.1(2)	0.35(7)	0.14(4)
	50.5	2.94	16.3	18.7(6)	4.21(15)	0.27(4)	7.8(9)	2.0(3)	0.24(5)	0.11(3)
$^{88}_{38}$Sr	42	2.73	25.5	16.6	3.18	0.37	5.34	2.86	0.20	0.086
$^{90}_{40}$Zr	42	2.74	22.6	19.5	-	-	-	-	0.25	0.082
	43	2.73	22.7	19.5	3.85	0.66	8.35	0.314	0.14	0.050
	50.1(5)	2.98	20.6	19.7(7)	4.0(2)	0.271(4)	7.3(10)	1.730(5)	0.144(8)	0.051(5)
$^{92}_{40}$Zr	43	2.76	22.2	20.0	4.46	0.53	13.6	0.189	0.183	0.065
$^{94}_{40}$Zr	43	2.76	23.8	18.5	4.48	0.60	11.7	1.88	0.168	0.071
	50.1(5)	2.99	20.3	19.9(7)	4.3(2)	0.389(6)	8.3(12)	2.071(5)	0.230(9)	0.081(7)
$^{92}_{42}$Mo	38.0	2.60	31.4	15.3(4)	3.1(6)	0.42(11)	6.5(15)	2.9(2)	0.12(1)	0.048(6)
	31	2.35	40.6	12.9	3.00	0.677	6.28	0.372	0.129	0.058
	49.2	2.96	21.2	20.2(7)	4.2(2)	0.371(9)	7.5(11)	1.228(5)	0.24(4)	0.087
$^{94}_{42}$Mo	50.5	3.00	21.2	20.0(7)	4.3(2)	0.41(1)	8.7(15)	1.142(5)	0.27(5)	0.095
$^{96}_{42}$Mo	45.0	2.83	25.0	17.9(6)	3.0(2)	0.34(1)	4.0(7)	0.90(29)	-	-
$^{98}_{42}$Mo	40	2.68	29.0	16.2	3.30	0.702	7.25	0.068	-	-
	45.0	2.84	23.2	19.3(7)	4.4(3)	0.43(2)	10.4(24)	1.6(3)	0.30(10)	0.099
$^{100}_{42}$Mo	38.0	2.61	29.1	16.6(6)	4.1(5)	0.54(11)	15.7(27)	2.2(2)	0.36(2)	0.14(1)
$^{106}_{46}$Pd	38.0	2.60	31.1	17.4(9)	4.0(6)	1.04(25)	10.5(23)	1.7(3)	0.45(7)	0.16(4)
$^{112}_{50}$Sn	44	2.82	29.6	18.1	4.57	0.88	9.9	2.2	0.21	0.069
	50.1	3.01	24.7	20.4(7)	4.5(2)	0.41(1)	14(3)	1.3(4)	0.22(13)	0.073
$^{114}_{50}$Sn	44	2.82	26.5	20.3	4.8	1.05	9.4	1.21	0.17	0.055
	50.1	3.01	24.4	20.7(8)	4.1(2)	0.313(9)	9.1(20)	1.294(5)	0.20(5)	0.064
$^{116}_{50}$Sn	40	2.68	33.8	17.0	3.75	0.49	8.9	0.334	0.26	0.0975
	40.4	2.70	30.2	18.5(6)	4.8(3)	0.90(5)	20(5)	1.488(5)	0.18(8)	0.055
	44	2.82	24.0	17.6	3.7	0.45	6.12	2.88	0.202	0.0944
$^{118}_{50}$Sn	40	2.68	35.3	16.3	3.5	0.54	6.8	1.07	0.24	0.094
	44	2.82	26.8	20.0	3.8	0.77	5.3	0.65	0.205	0.0699
$^{120}_{50}$Sn	40	2.68	34.6	16.6	3.6	0.56	6.1	1.14	0.26	0.099
	44	2.82	27.7	19.3	4.0	0.68	7.4	1.07	0.203	0.0719
	50.5	3.02	25.1	20.0(7)	3.9(2)	0.450(9)	6.5(11)	0.500(5)	0.22(11)	0.073
$^{122}_{50}$Sn	40	2.68	35.8	16.1	3.7	0.62	7.2	2.04	0.26	0.102
	44	2.82	30.5	17.5	3.9	0.52	6.5	0.515	0.192	0.0754
$^{124}_{50}$Sn	44	2.83	30.4	17.6	4.18	0.813	7.21	3.34	0.178	0.070
	50.5	3.03	22.9	22.0(8)	4.6(2)	0.48(1)	11(2)	2.042(5)	0.15(8)	0.043
$^{122}_{52}$Te	42	2.76	33.4	16.9	4.2	0.67	13.5	0.376	0.321	0.11
$^{124}_{52}$Te	42	2.76	33.1	17.1	4.2	0.60	13.9	0.195	0.283	0.099
$^{126}_{52}$Te	42	2.76	-	-	-	-	-	-	0.22	-
$^{128}_{52}$Te	42	2.77	32.9	17.2	4.1	0.78	12.1	0.425	0.195	0.066
$^{130}_{52}$Te	42	2.77	33.0	17.1	4.2	0.68	12.1	0.765	0.186	0.062
$^{140}_{58}$Ce	42	2.77	30.8	20.6	-	-	-	-	0.30	0.14
$^{148}_{62}$Sm	50	3.03	26.9	23.2	5.57	0.555	37.0	1.07	0.141	0.043
$^{152}_{62}$Sm	50	3.03	27.2	22.9	6.05	0.811	39.5	1.51	0.290	0.091
$^{154}_{62}$Sm	50	3.03	27.6	22.6	5.90	0.784	33.3	0.43	0.358	0.113
$^{166}_{68}$Er	50	3.04	29.7	22.9	6.13	0.959	48.9	1.63	0.294	0.083
$^{176}_{70}$Yb	50	3.04	30.2	23.2	5.98	0.863	49.3	1.82	0.285	0.085

Notes:

[1)]For references to the literature data, see the review of Ref. 20.

[2)]See the notes to Table II.

$$|C_n(I)|^2=\frac{4\pi(n!)^2}{k^{2n}(2I+1)(\theta^2-\theta_c^2)^n}\frac{[\sigma_I^{(n)}(\theta)]_{\max}}{[\sigma_0^{(0)}(\theta)]_{\max}}, \quad (16)$$

where $|\sigma_0^{(0)}(\theta)|_{\max}$ and $|\sigma_I^{(n)}(\theta)|_{\max}$ are the envelopes through the peaks of the elastic and inelastic scattering cross sections, and $\theta_c=2\tan^{-1}n/l_0$ is the Coulomb anglecorresponding to the trajectory that grazes the nuclear surface. On the basis of a systematization of the experimental data, it was shown in Ref. 13 that the nuclear matrix elements $|C_1(2)|$ are independent of the scattering angle θ and the energy E_α of the incident particles, i.e., it was shown that this quantity is indeed a nuclear constant. Table III gives the experimentally found parameters of the method of complex angular momenta, the nuclear matrix elements, and the absolute values of the quadrupole deformation parameters.

Use of anomalies in diffraction angular distributions to obtain the signs of the nuclear quadrupole deformation from experiments

A method widely used to find the signs of the nuclear quadrupole deformation from the angular distributions of the differential cross sections is the coupled-channel method (CCM),[27] which has been realized practically, for example, in the form of the well-known program ECIS.[28] In the coupled-channel method, the sign of the deformation is one of numerous adjustable parameters, and therefore the extraction of it from experiments is an ambiguous and unreliable procedure. In our study of Ref. 29, in which fitting using the ECIS program was employed, it was shown, nevertheless, that the sign of the nuclear deformation affects the shape of the angular distributions mainly by shifting the extrema to larger or smaller angles.

However, this shift of the extrema was predicted theoretically much earlier—in 1966 by Inopin and Shebeko—and it was found experimentally in experiments using the cyclotron of the Institute of Nuclear Physics of the Kazakh Academy of Sciences in 1971 (Ref. 30) and is now known in the literature as the "Blair phase-shift effect."[31,32] The strong interest in this effect is due to the fact that theoretically the magnitude and sign of the Blair phase shift β_2 were uniquely related to the magnitude and sign of the nuclear quadrupole deformation β_2 (Ref. 10) and also to the deformations of higher multipolarity in excitations of corresponding collective levels and measurement of their angular distributions of the differential cross sections in α-particle scattering. A complete review of investigations of the Blair phase shift was given in Ref. 9.

In the framework of the theory of inelastic diffraction scattering with excitation of collective nuclear levels,[33] the Blair phase-shift effect is interpreted as a contribution of higher orders in the nuclear deformation to the scattering amplitude.[10] To study this effect, Inopin and Shebeko[10] obtained scattering amplitudes without expanding the S matrix in powers of the nuclear deformation:

$$f_{I,M}(\theta)=i^I D_{M0}^{(I)}\left(\frac{\pi+\theta}{2}\right)f_I(\theta), \quad (17)$$

where

$$f_I(\theta)=\frac{1}{ik}\sum_{\bar{l}}\sqrt{\pi(2\bar{l}+1)}\,T_{\bar{l}}^{I}\,Y_{\bar{l}I}(\theta,0), \quad (18)$$

I and M are the spin and its projection in the final state of the nucleus, $\bar{l}$ is the mean angular momentum over the width of the packet of partial waves, $D_{M0}^{(I)}$ is a function of the irreducible representation of the rotation group, $T_{\bar{l}}^{I}$ are the matrix elements corresponding to excitation of levels with spin I, and $Y_{\bar{l}I}(\theta,0)$ are spherical functions. The amplitude (17) together with the amplitude for elastic scattering can be reduced to the form

$$\begin{aligned} f_0(\theta)&=F(\theta)\cos[kR_0\theta+\gamma],\\ f_2(\theta)&=-k\Delta_2\theta F(\theta)\sin[(kR_0+\delta_2)\theta+\gamma], \end{aligned} \quad (19)$$

where

$$F^2(\theta)=8\pi k^{-2}|a|^2 l_0\sin^{-1}\theta e^{-2\beta\theta}, \quad (20)$$

$$kR_0=l_0+\tfrac{1}{2}, \quad (21)$$

$$\Delta_2=\frac{R_0}{3}\frac{3}{\sqrt{4\pi}}\beta_2, \quad (22)$$

$$\delta_2=\frac{\sqrt{5}}{7\sqrt{4\pi}}kR_0\beta_2, \quad (23)$$

and l_0, β, b, $|a|$, γ are free parameters of the theory.

Since, as can be seen from Eq. (23), the quantity δ_2, being measured in an experiment, gives direct information about the sign of the nuclear quadrupole deformation,

$$\operatorname{sign}\beta_2=-\operatorname{sign}\delta_2, \quad (24)$$

we used the Blair phase shift for this purpose.

Thus, for practical calculations it is necessary to determine from experimental data the six free parameters of the theory: l_0, β, b, $|a|$, γ, δ_2, which occur in the expressions (17)–(23). We emphasize especially that the parameter δ_2 must be extracted together with its sign: sign δ_2. The first five parameters can be determined, as noted above, by the method proposed in Refs. 13 and 25. Without going into detailed descriptions of the method, we merely mention one remarkable feature of the method of complex angular momenta—the parameters of this theory can be determined uniquely from experiment, a considerable advantage of the method over the coupled-channel method. Systematized values of the parameters are given in Table III.

Methods of extracting the Blair phase shifts from experimental data are described in detail in Ref. 24. The most universal and reliable method is as follows. The value of δ_2 can be obtained not only from an extremum of the diffraction angular distribution of the differential cross sections but also from any point by using the expression (19) for the amplitude:

$$\delta_2=[\arcsin(\sqrt{\sigma(\theta)}/k\Delta_2\theta F(\theta))-\gamma]/\theta-kR_0, \quad (25)$$

$$\sigma(\theta)=|f_{IM}(\theta)|^2. \quad (26)$$

To eliminate from the calculations "spurious" theoretical free parameters, it is best to use in the expression (25), not the inelastic scattering cross section, but the ratio of it to the elastic cross section, since the same parameters are used in both amplitudes.

In the practical use of the Blair phase-shift method, one of the rigorous methodological conclusions was the following. When the Blair phase shift is used, the important thing is to choose correctly the region of angles in which the method of complex angular momenta works (Fraunhofer region). In practical calculations, it was found that this range of angles is very narrow: On the side of small angles it is limited by the Coulomb interaction, and also by Coulomb–nuclear interference, and on the side of large angles it is restricted by the region of change of the phase shifts by $\pi/2$.[12] Thus, with few exceptions we are in practice restricted to the region of the fourth and fifth diffraction peaks.

The results of measurements of the signs of the nuclear deformation by the coupled-channel method and the Blair phase-shift method are given in Table IV[10111213] in a comparison with literature data and a systematization. The parameter δ_2 and other intermediate quantities obtained from the experimental angular distributions of the differential cross sections are described in detail in our studies of Refs. 9 and 24.

3. THE NUCLEAR DEFORMATION SURFACE $\beta(Z,N)$ OF THE GROUND STATE OF NUCLEI WITH $Z=2$–102

The systematic study of the isotopic variations of nuclear shapes is one of the effective ways of recovering the surface $\beta(Z,N)$ as a whole in the complete Z, N region of existence of nuclei, from which one can then establish the fundamental trends of these variations. Since there are few stable nuclei in the complete region of existence of nuclei with any Z (short isotopic chains), the surface $\beta(Z,N)$ can be constructed in two ways: 1) experimentally, by means of data obtained by various experimental methods (Blair phase-shift, coupled-channel, conversion from Q, $B(E2)$, etc.); 2) by calculation if some model gives a reliable analytical relation between the nuclear deformation parameter and one of the quantities that can be measured accurately in nuclear spectroscopy, mainly the energies of the lowest, especially collective levels. Here, we shall not consider the numerous purely theoretical calculations of $\beta(Z,N)$, for example, those in Refs. 1 and 8, for the reasons indicated above (the uncontrollable variations of the results when there are small variations of the free parameters and the uncontrollable acccuracy of the assumptions and approximations that are made), although the data in the literature do undoubtedly exhibit a correlation between the purely theoretical and experimental functions $\beta(Z,N)$.

Numerous attempts to construct $\beta(Z,N)$ by the first method, for example, in Refs. 9 and 34, did not lead to success for two main reasons—the restricted number of experimental data and the discrepancy, sometimes contradiction, of the experimental data obtained from different reactions or by different methods. As an example, we give Table V, which compares the nuclear matrix elements (16) if one has in mind their connection with the nuclear deformation in the form (14), $|C_1(I)|$, obtained from different nuclear processes in which 2^+ and 3^- collective states are excited. It can be seen from Table V that the probabilities of the same transitions measured in different nuclear reactions agree satisfactorily on the whole, although there are significant differences. The establishment of the nature of these discrepancies is a task for the future, possibly the very distant future.

It is appropriate to give one further example. Let us consider the electric quadrupole moment Q and the quadrupole deformation parameter β_2. The first of them is related to the deformation of the charge component of the nucleus, and the second to the deformation of the mass component. There is a well known[43] relation between the intrinsic quadrupole moment Q_0 and the quadrupole deformation parameter:

$$Q_0=\tfrac{1}{132}ZR^2\beta_2. \tag{27}$$

However, it is difficult to establish the correspondence between the experimental values of Q_0 and β_2. First, Q_0 is not measured in an experiment, and the mean quadrupole moment Q for nuclei with $I=0$ or $1/2$ is zero. Second, the collective and single-particle excitations of nuclei are coupled and are separated only in even–even nuclei, in which the minimum energy of the single-particle levels is, owing to the pairing effect, ~ 2 MeV, while the energy of the collective excitations is somewhat less.[44] In odd and odd–odd nuclei, these excitations have comparable energies and the adiabatic conditions are not well satisfied. For this reason, the overwhelming bulk of the experimental data on elastic scattering of α particles relates to even–even nuclei. In addition, shell effects have a large influence on the values of Q_0 and β_2,[45] and therefore a correlation can be traced only within shells.

Let $\beta_z(A,S)$ and $\beta_m(A,S)$ be the deformations of the charge and mass components of the nuclei, respectively; they are functions of the mass number A and S, which is a measure of the filling of a shell. It is interesting to trace two types of correlation—the functional one between $\beta_z(A,S)$ and $\beta_m(A,S)$ and the correlation in the absolute magnitude $\beta_z(\beta_m)\,|_{\substack{A=\text{const}\\S=\text{const}}}$. To this end, we ascribe to nuclei with measured values of Q and β_2 a definite configuration, and, using the experimental values of Q, we calculate the parameter $\beta_z(A,S)$. These data for the shell $f_{7/2}$ are given in Table VI, and the functions $\beta_z(A,S)$ and $\beta_m(A,S)$ are represented in Fig. 2 by the points and crosses, respectively, for the shells $p_{3/2}$, $d_{5/2}$, $d_{3/2}$, $2p_{3/2}$, $f_{5/2}$, $g_{9/2}$, $g_{7/2}$.

It can be seen from Fig. 2 that there is an obvious functional correlation of $\beta_z(A,S)$ and $\beta_m(A,S)$ in the shells $f_{7/2}$, $p_{3/2}$, $d_{5/2}$, $2p_{3/2}$, and $f_{5/2}$. For the shells $d_{3/2}$, $g_{9/2}$, and $g_{7/2}$ there were too few experimental data for such a conclusion. One can also give two examples of numerical correlation: The ^{7}Li nucleus in the shell $p_{3/2}$ has $\beta_z(7;1)=-1.29$, which should be compared with $\beta_m(7;1)=1.47$; the ^{27}Al nucleus in the shell $d_{5/2}$ has $\beta_z(27;5)=+0.23$, which should be compared with $\beta_m(27;5)=0.13$. The elucidation of this correlation ap-

TABLE IV. The nuclear deformation surface $\beta(Z,N)$.

Nucleus	E^*_{2+}, MeV (Refs. 53–55)	β_2 (Ref. 60)	β_2^{exp} Value	β_2^{exp} Method	β_2^{theor}	β_2^{ref}	Surface $\beta(Z,N)$	Number of neutrons N
$^{4}_{2}$He	33.0						+0.172	2
^{6}He	1.80					+0.736 (From ^{8}Be)	+0.736	4
^{8}He								6
$^{6}_{4}$Be	1.67						+0.770	2
^{8}Be	2.94					+0.58 (From ^{9}Be)	+0.580	4
^{9}Be					+0.58		+0.580	5
^{10}Be	3.3680	1.22	0.74				+0.542	6
^{12}Be	0.8						+1.11	8
$^{10}_{6}$C	3.353		+0.4	Extrapol.			+0.334	4
^{12}C	4.4391	0.60	−0.29(2)	BPSM		−0.29	−0.290	6
^{13}C			−0.19(4)	BPSM			−0.190	7
^{14}C	7.012				−0.44		−0.231	8
^{16}C	1.75				+0.37		+0.462	10
^{18}C					+0.39		+0.390	12
^{20}C					−0.55		−0.550	14
^{22}C					+0.37		+0.370	16
^{24}C					−0.62		−0.620	18
$^{14}_{8}$O	6.59						+0.0861	6
^{16}O	6.919	0.084	+0.18(3)	BPSM		+0.084	+0.0840	8
^{18}O	1.9822	0.30					+0.157	10
^{20}O	1.6737						+0.171	12
$^{18}_{10}$Ne	1.8873						+0.325	8
^{20}Ne	1.6338	0.87	+0.35(1)	CCM	+0.349	+0.35	+0.350	10
^{22}Ne	1.27458	0.64	+0.37(1)	CCM			+0.397	12
^{24}Ne	1.981						+0.318	14
$^{20}_{12}$Mg			+0.4	Extrapol.				8
^{22}Mg	1.2470		+0.6	Extrapol.			+0.639	10
^{24}Mg	1.36859	0.65	+0.61(5)	BPSM	+0.26:0.47	+0.61	+0.610	12
^{26}Mg	1.8087		+0.28(1)	CCM	+0.19		+0.531	14
^{28}Mg	1.4735		+0.2	Extrapol.			+0.589	16
$^{26}_{14}$Si	1.7959						−0.358	12
^{28}Si	1.7789	0.40	−0.36(3)	BPSM	$-\beta$	−0.36	−0.360	14
^{30}Si	2.2355						−0.321	16
^{32}Si	1.9414						−0.345	18
$^{30}_{16}$S	2.2107						−0.211	14
^{32}S	2.2302	0.37	−0.30	CCM	−0.20	−0.21	−0.210	16
^{34}S	2.1274		0.27	DWM*			−0.215	18
^{36}S	3.291						−0.173	20
$^{34}_{18}$Ar	2.0911						−0.167	16
^{36}Ar	1.97039		−0.36	CCM	$-\beta$		−0.172	18
^{38}Ar	2.16760		0.17	DWM			−0.164	20
^{40}Ar	1.46081		0.20	DWM		−0.20	−0.200	22
^{42}Ar	1.2082						−0.220	24
$^{38}_{20}$Ca	2.206						+0.106	18
^{40}Ca	3.9041		0.08	DWM	$\beta=0$	+0.08	+0.0800	20
^{42}Ca	1.5246		0.19	DWM	$\beta=0$		+0.128	22
^{44}Ca	1.15702	0.22	+0.17	BPSM	$\beta=0$		+0.147	24
^{46}Ca	1.347		0.28	DWM	$\beta=0$		+0.136	26
^{48}Ca	3.8323		+0.11	BPSM	$\beta=0$		+0.0807	28
^{50}Ca	1.03						+0.156	30
$^{42}_{22}$Ti	1.555						+0.151	20
^{44}Ti	1.0830				$+\beta$		+0.181	22
^{46}Ti	0.88925	0.29	+0.19(1)	CCM	$+\beta$		+0.200	24
^{48}Ti	0.983512	0.265	+0.19(1)	CCM	$+\beta$	+0.19	+0.190	26
^{50}Ti	1.5537	0.175	+0.13(1)	CCM	$\beta=0$		+0.151	28
^{52}Ti	1.0471						+0.184	30
$^{48}_{24}$Cr	0.7524				$+\beta$		+0.242	24
^{50}Cr	0.7833	0.31			$+\beta$		+0.238	26
^{52}Cr	1.43408	0.23			$\beta=0$		+0.176	28
^{54}Cr	0.83483	0.27	+0.23(2)	BPSM	$+\beta$	+0.23	+0.230	30
^{56}Cr	1.008						+0.209	32
$^{52}_{26}$Fe	0.84				$+\beta$		+0.211	26

TABLE IV. (*Continued.*)

Nucleus	E^*_{2+}, MeV (Refs. 53–55)	β_2 (Ref. 60)	β_2^{exp} Value	β_2^{exp} Method	β_2^{theor}	β_2^{ref}	Surface $\beta(Z,N)$	Number of neutrons N
^{54}Fe	1.4084	0.18	+0.12(3)	BPSM	β=0		+0.163	28
^{56}Fe	0.84676	0.23	+0.21	BPSM	+β	+0.21	+0.210	30
^{58}Fe	0.81076	0.27	+0.14	BPSM	+β		+0.215	32
^{60}Fe	0.84						+0.211	34
^{62}Fe	1.63						+0.151	36
$^{56}_{28}$Ni	2.701				β=0		+0.125	28
^{58}Ni	1.4544	0.187	+0.17(2)	BPSM	−0.171	+0.17	+0.170	30
^{60}Ni	1.33250	0.211	−0.21(3)	BPSM	−0.170		−0.178	32
^{62}Ni	1.1730	0.193	+0.20(2)	BPSM	+0.190		+0.189	34
^{64}Ni	1.3461	0.192	−0.14(2)	BPSM	−0.189		−0.176	36
^{66}Ni	1.42						−0.172	38
$^{60}_{30}$Zn	1.0042						−0.189	30
^{62}Zn	0.9539						−0.194	32
^{64}Zn	0.9915	0.250	−0.19(2)	BPSM	−0.108	−0.19	−0.190	34
^{66}Zn	1.0394	0.227	−0.12(2)	BPSM	−0.0980		−0.186	36
^{68}Zn	1.0774	0.205	−0.23(2)	BPSM	−0.0900		−0.183	38
^{70}Zn	0.8848	0.229	−0.15(3)	BPSM	0.123		−0.201	40
^{72}Zn	0.65						−0.235	42
$^{64}_{32}$Ge					−β			32
^{66}Ge	0.9574				β=0		−0.189	34
^{68}Ge	1.0165				−β		−0.183	36
^{70}Ge	1.0396	0.224			0.201		−0.182	38
^{72}Ge	0.83395	0.247			−0.218		−0.203	40
^{74}Ge	0.59588	0.290	+0.24(3)	BPSM	0.226	+0.24	+0.240	42
^{76}Ge	0.56293	0.271			0.204		+0.247	44
^{78}Ge					0.195			46
$^{72}_{34}$Se	0.8620						+0.211	38
^{74}Se	0.6348	0.337			+0.32		+0.246	40
^{76}Se	0.5591	0.326			0.228		+0.262	42
^{78}Se	0.6136	0.287			0.190		+0.250	44
^{80}Se	0.6662	0.240			0.166	+0.24	+0.240	46
^{82}Se	0.6544	0.205			0.0713		+0.242	48
^{84}Se	1.4551						+0.162	50
^{86}Se	0.704						+0.233	52
$^{74}_{36}$Kr	0.4557						+0.291	38
^{76}Kr	0.4238						+0.301	40
^{78}Kr	0.4550				0.267		+0.291	42
^{80}Kr	0.6162				0.188		+0.250	44
^{82}Kr	0.77649				0.149		+0.223	46
^{84}Kr	0.88160				0.0700	+0.209 (From ^{80}Se)	+0.209	48
^{86}Kr	0.5649						+0.261	50
^{88}Kr	0.7753						+0.223	52
^{90}Kr	0.7071						+0.233	54
$^{78}_{38}$Sr	0.505						+0.164	40
^{80}Sr	0.3854						+0.188	42
^{82}Sr	0.5734						+0.154	44
^{84}Sr	0.7931						+0.131	46
^{86}Sr	1.0766				0.0500		+0.112	48
^{88}Sr	1.83603	0.140	+0.086	BPSM	0.0707	+0.086	+0.0860	50
^{90}Sr	0.83169						+0.128	52
^{92}Sr	0.8147						+0.129	54
^{94}Sr	0.8374						+0.128	56
^{96}Sr							+0.129	58
$^{88}_{40}$Zr	1.0569						+0.106	48
^{90}Zr	2.18622	0.074			0.0782	+0.074	+0.0740	50
^{92}Zr	0.9345	0.11			0.00504		+0.113	52
^{94}Zr	0.9188				0.110		+0.114	54
^{96}Zr	1.751	0.081					+0.0828	56
^{98}Zr	0.8530						+0.119	58
^{100}Zr	0.2125						+0.237	60
^{102}Zr	0.1519						+0.281	62
$^{90}_{42}$Mo	0.948						−0.0606	48
^{92}Mo	1.50947	0.116	−0.048(6)	BPSM	0.0795	−0.048	−0.0480	50

TABLE IV. (*Continued.*)

Nucleus	E^*_{2+}, MeV (Refs. 53–55)	β_2 (Ref. 60)	β_2^{exp} Value	β_2^{exp} Method	β_2^{theor}	β_2^{ref}	Surface $\beta(Z,N)$	Number of neutrons N
^{94}Mo	0.87110	0.169			0.00975		+0.0632	52
^{96}Mo	0.77822	0.175			0.117		+0.0869	54
^{98}Mo	0.78737	0.168			0.131		+0.0665	56
^{100}Mo	0.5352	0.253	+0.14(1)	BPSM	0.175		+0.0806	58
^{102}Mo	0.2960						+0.108	60
^{104}Mo	0.1920						+0.135	62
^{106}Mo	0.1717						+0.142	64
$^{94}_{44}$Ru	1.428						+0.152	50
^{96}Ru	0.8326	0.159			0.0126		+0.199	52
^{98}Ru	0.65241	0.215			0.110		+0.225	54
^{100}Ru	0.53959	0.232			0.147		+0.248	56
^{102}Ru	0.47506	0.264			0.165	+0.264	+0.264	58
^{104}Ru	0.35799	0.288			0.198		+0.304	60
^{106}Ru	0.2703						+0.350	62
^{108}Ru	0.2424						+0.370	64
^{110}Ru	0.24067						+0.371	66
^{112}Ru	0.2368						+0.374	68
$^{98}_{46}$Pd	0.8413						+0.125	52
^{100}Pd	0.6658						+0.140	54
^{102}Pd	0.55660						+0.153	56
^{104}Pd	0.55581	0.212			0.141		+0.154	58
^{106}Pd	0.51186	0.224	+0.16(4)	BPSM	0.149	+0.160	+0.160	60
^{108}Pd	0.43393	0.243			0.189		+0.174	62
^{110}Pd	0.3738	0.252			0.194		+0.187	64
^{112}Pd	0.3489						+0.194	66
^{114}Pd	0.3329						+0.198	68
^{116}Pd	0.3406						+0.196	70
$^{102}_{48}$Cd	0.719						+0.170	54
^{104}Cd	0.6581						+0.178	56
^{106}Cd	0.6327	0.186			0.133		+0.181	58
^{108}Cd	0.63298	0.195			0.131		+0.181	60
^{110}Cd	0.65775	0.183			0.0940		+0.178	62
^{112}Cd	0.6174	0.186			0.0966		+0.184	64
^{114}Cd	0.55829	0.193			0.101	+0.193	+0.193	66
^{116}Cd	0.51355	0.201			0.104		+0.201	68
^{118}Cd	0.4878						+0.206	70
^{120}Cd	0.5059						+0.206	72
^{122}Cd	0.570						+0.191	74
$^{102}_{50}$Sn	1.354						−0.112	52
^{104}Sn	1.2162						−0.118	54
^{106}Sn	1.2104						−0.118	56
^{108}Sn	1.2067						−0.118	58
^{110}Sn	1.2117						−0.118	60
^{112}Sn	1.2572	0.130	−0.069	BPSM	0.113		−0.116	62
^{114}Sn	1.3000	0.118	−0.055	BPSM	0.115		−0.114	64
^{116}Sn	1.29354	0.113	−0.13	BPSM	0.115		−0.114	66
^{118}Sn	1.2296	0.116	−0.10	BPSM	0.111		−0.117	68
^{120}Sn	1.1716	0.112	−0.12	BPSM	0.102	−0.120	−0.120	70
^{122}Sn	1.1411	0.118	−0.13	BPSM	0.0948		−0.122	72
^{124}Sn	1.132	0.108			0.0891		−0.122	74
^{126}Sn	1.145						−0.121	76
^{128}Sn								78
^{130}Sn	1.217						−0.118	80
$^{112}_{52}$Te	0.720						+0.130	60
^{114}Te	0.7090						+0.131	62
^{116}Te	0.6791						+0.133	64
^{118}Te	0.6052						+0.141	66
^{120}Te	0.5604	0.170					+0.147	68
^{122}Te	0.5640	0.183	+0.20	BPSM			+0.146	70
^{124}Te	0.60272	0.174	+0.18	BPSM			+0.142	72
^{126}Te	0.66633	0.163	+0.17	BPSM			+0.135	74
^{128}Te	0.7432	0.141	+0.15	BPSM			+0.128	76
^{130}Te	0.8394	0.127	+0.12	BPSM		+0.120	+0.120	78
^{132}Te	0.9739						+0.111	80

TABLE IV. (*Continued.*)

Nucleus	E^*_{2+}, MeV (Refs. 53–55)	β_2 (Ref. 60)	β_2^{exp} Value	β_2^{exp} Method	β_2^{theor}	β_2^{ref}	Surface $\beta(Z,N)$	Number of neutrons N
^{134}Te	1.2791						+0.0972	82
$^{116}_{54}$Xe	0.337						+0.163	62
^{118}Xe	0.337						+0.163	64
^{120}Xe	0.3218						+0.167	66
^{122}Xe	0.3315						+0.165	68
^{124}Xe	0.3543						+0.159	70
^{126}Xe	0.38863	0.190					+0.152	72
^{128}Xe	0.44288	0.171					+0.142	74
^{130}Xe	0.53609						+0.129	76
^{132}Xe	0.6677	0.116				+0.116	+0.116	78
^{134}Xe	0.84702						+0.103	80
^{136}Xe	1.3131						+0.0828	82
^{138}Xe	0.5895						+0.123	84
^{140}Xe	0.3768						+0.154	86
$^{120}_{56}$Ba	0.183						−0.337	64
^{122}Ba	0.197						−0.324	66
^{124}Ba	0.2296						−0.300	68
^{126}Ba	0.256				$-\beta$		−0.285	70
^{128}Ba	0.283	0.175					−0.271	72
^{130}Ba	0.3573	0.170			$-\beta$		−0.241	74
^{132}Ba	0.46455						−0.211	76
^{134}Ba	0.60470				$-\beta$		−0.185	78
^{136}Ba	0.81850				$-\beta$		−0.159	80
^{138}Ba	1.4359	0.120			$-\beta$	−0.120	−0.120	82
^{140}Ba	0.60232						−0.186	84
^{142}Ba	0.35952						−0.240	86
^{144}Ba	0.1994						−0.323	88
^{146}Ba	0.1810						−0.338	90
$^{128}_{58}$Ce	0.2073						−0.289	70
^{130}Ce	0.2539						−0.261	72
^{132}Ce	0.3250						−0.231	74
^{134}Ce	0.4092						−0.206	76
^{136}Ce	0.5522						−0.177	78
^{138}Ce	0.7887						−0.148	80
^{140}Ce	1.59617	0.104				−0.104	−0.104	82
^{142}Ce	0.6412	0.118					−0.164	84
^{144}Ce	0.3973						−0.209	86
^{146}Ce	0.2586						−0.258	88
^{148}Ce	0.1587						−0.330	90
^{150}Ce	0.098						−0.420	92
$^{128}_{60}$Nd	0.144						−0.244	68
^{130}Nd								70
^{132}Nd								72
^{134}Nd	0.2942						−0.171	74
^{136}Nd	0.3735						−0.151	76
^{138}Nd	0.5202						−0.128	78
^{140}Nd	0.7738						−0.105	80
^{142}Nd	1.5758	0.104					−0.0737	82
^{144}Nd	0.69649	0.111			$\beta=0$	−0.111	−0.111	84
^{146}Nd	0.4538	0.161					−0.137	86
^{148}Nd	0.3017	0.197			$\beta=0$		−0.169	88
^{150}Nd	0.1301	0.268					−0.257	90
^{152}Nd	0.0759						−0.336	92
^{154}Nd	0.0728						−0.343	94
$^{140}_{62}$Sm	0.5310						+0.120	78
^{142}Sm	0.7680						+0.0996	80
^{144}Sm	1.6601						+0.0678	82
^{146}Sm	0.7471						+0.101	84
^{148}Sm	0.5501	0.158	+0.11	BPSM			+0.118	86
^{150}Sm	0.33395	0.187			$\beta=0$		+0.151	88
^{152}Sm	0.12178	0.294	+0.25	BPSM		+0.250	+0.250	90
^{154}Sm	0.08199	0.326	+0.27	BPSM			+0.305	92
^{156}Sm	0.0760						+0.317	94
^{158}Sm	0.0728						+0.324	96

TABLE IV. (*Continued.*)

Nucleus	E^*_{2+}, MeV (Refs. 53–55)	β_2 (Ref. 60)	β_2^{exp} Value	β_2^{exp} Method	β_2^{theor}	β_2^{ref}	Surface $\beta(Z,N)$	Number of neutrons N
$^{142}_{64}$Gd	0.5260						+0.130	78
^{144}Gd	0.7426						+0.110	80
^{146}Gd								82
^{148}Gd	0.7845						+0.107	84
^{150}Gd	0.6381						+0.118	86
^{152}Gd	0.3443	0.184					+0.161	88
^{154}Gd	0.12307	0.293					+0.269	90
^{156}Gd	0.088964	0.325					+0.317	92
^{158}Gd	0.07951	0.335				+0.335	+0.335	94
^{160}Gd	0.07526	0.343					+0.344	96
$^{150}_{66}$Dy	0.8044						+0.0981	84
^{152}Dy	0.6140						+0.112	86
^{154}Dy	0.3345						+0.152	88
^{156}Dy	0.1379	0.282					+0.237	90
^{158}Dy	0.09892	0.307					+0.280	92
^{160}Dy	0.080660	0.320					+0.299	94
^{162}Dy	0.080660	0.320					+0.310	96
^{164}Dy	0.073392	0.325			$+\beta$	+0.325	+0.325	98
$^{156}_{68}$Er	0.3446						+0.135	88
^{158}Er	0.1921	0.234					+0.181	90
^{160}Er	0.1257	0.286					+0.224	92
^{162}Er	0.10200	0.304					+0.249	94
^{164}Er	0.09139	0.318					+0.263	96
^{166}Er	0.08057	0.322	+0.28	**BPSM**		+0.280	+0.280	98
^{168}Er	0.079800	0.321					+0.281	100
^{170}Er	0.07859	0.317					+0.284	102
$^{158}_{70}$Yb	0.358						+0.134	88
^{160}Yb	0.2430						+0.163	90
^{162}Yb	0.1663						+0.197	92
^{164}Yb	0.1233						+0.299	94
^{166}Yb	0.10238						+0.251	96
^{168}Yb	0.08773	0.304					+0.271	98
^{170}Yb	0.084262	0.308					+0.276	100
^{172}Yb	0.078746	0.315					+0.286	102
^{174}Yb	0.07647	0.305					+0.290	104
^{176}Yb	0.08213	0.292	+0.28	**BPSM**		+0.280	+0.280	106
$^{166}_{72}$Hf	0.1587						+0.201	94
^{168}Hf	0.1239						+0.227	96
^{170}Hf	0.1008						+0.252	98
^{172}Hf	0.09526	0.263					+0.259	100
^{174}Hf	0.09100	0.273					+0.265	102
^{176}Hf	0.08835	0.286					+0.269	104
^{178}Hf	0.09318	0.263					+0.262	106
^{180}Hf	0.093324	0.262				+0.262	+0.262	108
^{182}Hf	0.0978						+0.256	110
$^{170}_{74}$W	0.1560						+0.189	96
^{172}W	0.1229						+0.214	98
^{174}W	0.1119						+0.224	100
^{176}W	0.1089						+0.227	102
^{178}W	0.1059						+0.230	104
^{180}W	0.10365	0.243					+0.232	106
^{182}W	0.100106	0.238					+0.237	108
^{184}W	0.11121	0.225				+0.225	+0.225	110
^{186}W	0.12261	0.217					+0.214	112
^{188}W	0.143						+0.198	114
$^{172}_{76}$Os	0.2277						+0.159	96
^{174}Os	0.152						+0.194	98
^{176}Os	0.1352						+0.206	100
^{178}Os	0.1317						+0.209	102
^{180}Os	0.1318						+0.209	104
^{182}Os	0.1271						+0.213	106
^{184}Os	0.1198						+0.219	108
^{186}Os	0.13715	0.199					+0.205	110
^{188}Os	0.15504	0.186			0.199		+0.193	112

TABLE IV. (*Continued.*)

Nucleus	E^*_{2+}, MeV (Refs. 53–55)	β_2 (Ref. 60)	β_2^{exp} Value	β_2^{exp} Method	β_2^{theor}	β_2^{ref}	Surface $\beta(Z,N)$	Number of neutrons N
^{190}Os	0.18668	0.176			0.172		+0.175	114
^{192}Os	0.2057955	0.167			0.133	+0.167	+0.167	116
$^{178}_{78}$Pt	0.17						+0.211	100
^{180}Pt	0.16						+0.218	102
^{182}Pt	0.1549						+0.221	104
^{184}Pt	0.1630						+0.216	106
^{186}Pt	0.19153						+0.199	108
^{188}Pt	0.2656						+0.169	110
^{190}Pt	0.29582	0.158					+0.160	112
^{192}Pt	0.3165079	0.170			0.113		+0.155	114
^{194}Pt	0.32845	0.152			0.0869	+0.152	+0.152	116
^{196}Pt	0.3557	0.125			0.0580		+0.146	118
^{198}Pt	0.4072	0.134			0.0417		+0.136	120
$^{184}_{80}$Hg	0.3667						+0.0942	104
^{186}Hg	0.4053						+0.0896	106
^{188}Hg	0.4128						+0.0888	108
^{190}Hg	0.4164						+0.0884	110
^{192}Hg	0.4228						+0.0877	112
^{194}Hg	0.4282						+0.0872	114
^{196}Hg	0.4261	0.129					+0.0874	116
^{198}Hg	0.4118044	0.109					+0.0889	118
^{200}Hg	0.36794	0.098					+0.0940	120
^{202}Hg	0.43956	0.086				+0.086	+0.0860	122
^{204}Hg	0.4366	0.047					+0.0863	124
^{206}Hg	1.068						+0.0552	126
$^{194}_{82}$Pb	0.9642						+0.0338	112
^{196}Pb	1.0486						+0.0324	114
^{198}Pb	1.0634						+0.0322	116
^{200}Pb	1.0262						+0.0327	118
^{202}Pb	0.96067						+0.0338	120
^{204}Pb	0.8992	0.048					+0.0350	122
^{206}Pb	0.8031	0.037				+0.037	+0.0370	124
^{208}Pb								126
^{210}Pb	0.7997						+0.0371	128
^{212}Pb	0.8049						+0.0370	130
^{214}Pb	0.837						+0.0362	132
$^{200}_{84}$Po	0.668						+0.0405	116
^{202}Po	0.6753						+0.0403	118
^{204}Po	0.6833						+0.0400	120
^{206}Po	0.70066						+0.0395	122
^{208}Po	0.6865						+0.0399	124
^{210}Po	1.1814						+0.0305	126
^{212}Po	0.7273						+0.0388	128
^{214}Po	0.60931					+0.0424 (From ^{214}Pb)	+0.0424	130
^{216}Po	0.54973						+0.0446	132
^{218}Po	0.512						+0.0462	134
$^{206}_{86}$Rn	0.632						+0.0760	120
^{208}Rn								122
^{210}Rn	0.644						+0.0752	124
^{212}Rn	1.2723						+0.0536	126
^{214}Rn								128
^{216}Rn	0.465						+0.0885	130
^{218}Rn	0.32422	0.088					+0.106	132
^{220}Rn	0.24098	0.123				+0.123	+0.123	134
^{222}Rn	0.18618	0.136					+0.140	136
$^{214}_{88}$Ra	1.381						+0.0425	126
^{216}Ra	0.6879						+0.0602	128
^{218}Ra								130
^{220}Ra	0.177						+0.119	132
^{222}Ra	0.11112	0.183					+0.150	134
^{224}Ra	0.08437	0.172				+0.172	+0.172	136
^{226}Ra	0.06773	0.197					+0.192	138
^{228}Ra	0.059	0.211					+0.206	140

TABLE IV. (*Continued.*)

Nucleus	E^*_{2+}, MeV (Refs. 53–55)	β_2 (Ref. 60)	β_2^{exp} Value	β_2^{exp} Method	β_2^{theor}	β_2^{ref}	Surface $\beta(Z,N)$	Number of neutrons N
$^{224}_{90}$Th	0.093						+0.176	134
^{226}Th	0.07220	0.219					+0.200	136
^{228}Th	0.0578	0.223					+0.224	138
^{230}Th	0.05323	0.233				+0.233	+0.233	140
^{232}Th	0.04937	0.251					+0.242	142
^{234}Th	0.0495	0.232					+0.242	144
$^{228}_{92}$U	0.059						+0.192	136
^{230}U	0.0517	0.242					+0.205	138
^{232}U	0.0476	0.253					+0.214	140
^{234}U	0.04349	0.253					+0.224	142
^{236}U	0.04524	0.269					+0.219	144
^{238}U	0.04491	0.281	+0.22	CCM		+0.220	+0.220	146
^{240}U	0.045						+0.220	148
$^{236}_{94}$Pu	0.0446						+0.268	142
^{238}Pu	0.04408	0.267					+0.270	144
^{240}Pu	0.04282	0.274				+0.274	+0.274	146
^{242}Pu	0.04454	0.284					+0.269	148
^{244}Pu	0.045						+0.267	150
$^{238}_{96}$Cm	0.035						+0.349	142
^{240}Cm	0.04						+0.326	144
^{242}Cm	0.04212						+0.318	146
^{244}Cm	0.0429	0.315				+0.315	+0.315	148
^{246}Cm	0.042852						+0.315	150
^{248}Cm	0.04340						+0.313	152
^{250}Cm	0.043						+0.315	154
$^{244}_{98}$Cf	0.04						+0.367	146
^{246}Cf								148
^{248}Cf	0.042						+0.358	150
^{250}Cf	0.042721	0.355				+0.355	+0.355	152
^{252}Cf	0.04572						+0.343	154
$^{248}_{100}$Fm	0.044						+0.352	148
^{250}Fm								150
^{252}Fm								152
^{254}Fm	0.04499					+0.348 (From ^{250}Cf)	+0.348	154
^{256}Fm	0.0481						+0.337	156
$^{252}_{102}$No								150

*DWM: distorted-wave method.

Notes:

[1)]In the absence of experimental data, the data from the systematization of Ref. 60 were taken for β_{ref}.

[2)]In the absence of experimental data and data in the systematizations, the results from the nearest isobars were taken for β_{ref}.

[3)]In view of the large number of references to original studies, they are only given in part in the table; the remaining references can be found in Refs. 9, 14, 30, and 60–64.

*DWM: distorted-wave method.

pears to be an interesting subject for further experimental investigations in the region of inelastic scattering of α particles of medium energies by even and odd nuclei. Thus, it can be seen from Fig. 2 and Table VI that the deformations of the charge and mass components of nuclei are correlated, and sometimes agree in absolute magnitude and even sign. However, there are too few facts to know that the surface $\beta(Z,N)$ is the same for even and odd nuclei, or the even–odd difference are too large (and in sign may be opposite) to construct for them a single surface.

Thus, using the first method, one can hope to construct only fragments or individual segments of the complete surface $\beta(Z,N)$, and the surface itself over the complete range of existing nuclei must be recovered by the second method. For this there is already a reliable theoretical basis. We used the study of Ref. 47, which proposed an interpretation of the nuclear matrix elements $C_1(I)$ on the basis of the modern microscopic theory of nuclear structure. In contrast to many interpretations of the reduced probabilities $B(E2)$, which were obtained from experiments on Coulomb excitation,[48] the study of Ref. 47 considered nuclear matrix elements $C_1(2)$ corresponding to single-phonon quadrupole excitations of nuclei in inelastic scattering of α particles.

In the theory of inelastic scattering, the main task is to extract from the experimental angular distributions the nuclear structure factors associated with the nuclear deformation or the amplitude of vibrations of the nuclear surface and also with the wave functions of the nuclear states. The values of $|C_n(I)|^2$ occur as factors in the expressions for the cross sections for inelastic diffraction scattering with excitation of n-phonon nuclear states.[49] The study of

TABLE V. Nuclear matrix elements $|C_1(I)|$ obtained from different nuclear processes.

Nucleus	I^π	(α,α') (Refs. 9,13)	(α,α') (Ref. 35)	$(^3He,^3He')$ (Refs. 36,37)	(d,d') (Refs. 38,39)	(p,p') (Refs. 39,40)	(e,e') (Ref. 41)	Coul. exc. (Ref. 42)
^{24}Mg	2^+	0.78	0.62 Ref. (56)	-	-	-	-	0.77
^{28}Si	2^+	0.57	0.29 Ref. (57)	0.69	0.63	0.67	-	0.58
^{54}Fe	2^+	0.22	0.22	-	0.38	0.29	-	-
^{58}Ni	2^+	0.35	0.42	0.41	0.48	0.39	0.30	0.37
	3^-	0.21	0.23	0.26	0.22	-	0.18	-
^{60}Ni	2^+	0.40	0.48	0.47	0.53	-	0.31	0.42
	3^-	0.26	0.21	0.25	0.31	-	0.17	-
^{62}Ni	2^+	0.37	0.36	0.52	0.46	-	-	0.38
	3^-	0.27	0.21	0.27	0.31	-	-	-
^{64}Ni	2^+	0.34	0.40	0.53	0.42	0.45	0.32	-
	3^-	0.20	0.27	0.28	0.29	-	0.19	-
^{64}Zn	2^+	0.42	0.45	0.43	0.58	0.51	0.45	0.54
	3^-	0.26	0.28	-	0.44	0.42	0.21	-
^{68}Zn	2^+	0.46	0.39 (Ref. 58)	-	0.50	0.47	-	0.46
	3^-	0.27	0.27 (Ref. 58)	-	0.37	0.40	-	-
^{74}Ge	2^+	0.54	-	-	-	-	-	0.65
^{92}Mo	2^+	0.12	0.13 (Ref. 59)	-	-	-	-	-
^{100}Mo	2^+	0.36	-	-	-	-	-	0.62
^{106}Pd	2^+	0.45	-	-	-	-	-	0.58

Ref. 47 used a superfluid nuclear model taking into account pairing correlations and the quadrupole–quadrupole interaction of nucleons in open shells.

In Refs. 50 and 51, a comparison was made of the experimental data with the superfluid model in two different calculations: 1) The contribution of the nuclear core to the interaction was taken into account by means of effective mass neutron and proton charges q^n_{eff} and q^p_{eff} (Ref. 50); 2) the parameters q^ξ were not introduced, but it was assumed that the quadrupole–quadrupole interaction is effective between p–p and n–n nucleon pairs independently of the charge and the nucleon shell.[51]

In the first calculation, the formula for the nuclear matrix element has the form

TABLE VI. Charge and mass components of the nuclear quadrupole deformation parameter for nuclei belonging to the $f_{7/2}$ shell.

S	Even nucleus	Odd nucleus	β_m	β_Z
1	-	^{45}Sc	-	−0.11
2	^{42}Ca	-	0.15	-
3	-	^{51}V	-	+0.12
4	^{44}Ca	-	0.17	-
	^{54}Cr	-	+0.23	-
	^{56}Fe	-	0.21	-
5	-	^{55}Mn	-	+0.17
6	^{48}Ti	-	0.22	-
7	-	^{59}Co	-	+0.13
8	^{48}Ca	-	0.11	-
	^{54}Fe	-	−0.12	-

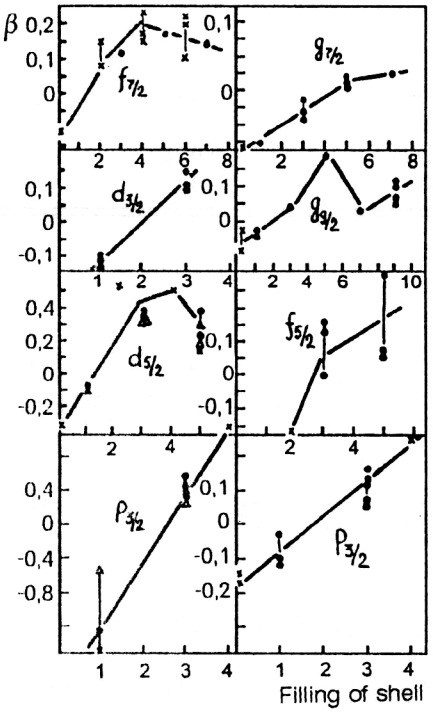

FIG. 2. Functional correlation between deformations of the charge and mass components of nuclei. The black circles give charge data, the crosses give mass data, and the black triangles were calculated in the generalized model of Ref. 46.

TABLE VII. Shape parameters of the nuclear surface of C and Mg isotopes.

Nucleus	I^π	β_2^{exp}	β_2^{theor}	Method	Reference
^{9}C	$(3/2^-)$	+0.4		Extrapolation	[65]
^{10}C	0^+	+0.4		Extrapolation	[65]
^{11}C	$3/2^-$	+0.41(1)		Calculated from Q	[53]
^{12}C	0^+	−0.30(2)		BPSM, 39 MeV	[65]
		−0.29(2)		BCSM, 50.5 MeV	[65]
		−0.29(2)		CCM, 104 MeV	[70]
		(0.3÷0.9)		Var. exp. meth.	[62]
			−0.33−0.42	Hartree–Fock	[71–73]
			−0.29	Variational	[74–76]
			−(0.45−0.67)	K harmonics	[77–82]
^{13}C	$1/2^-$	−0.19(4)		BCSM, 33.4 MeV	[65]
^{14}C	0^+		−0.44	Variational	[76]
^{15}C	$1/2^+$	−0.1		Interpolation	[65]
^{16}C	0^+		+0.37	Variational	[76]
^{17}C		+0.4		Interpolation	[65]
^{18}C			+0.39	Variational	[76]
^{19}C		0		Interpolation	[65]
^{20}C			−0.55	Variational	[76]
^{21}C		−0.1		Interpolation	[65]
^{22}C			+0.37	Variational	[76]
^{23}C		−0.2		Interpolation	[65]
^{24}C			−0.62	Variational	[76]
^{20}Mg	0^+	+0.4		Extrapolation	[65]
^{21}Mg	$5/2^+$	+0.5		Extrapolation	[65]
^{22}Mg	0^+	+0.6		Extrapolation	[65]
^{23}Mg	$3/2^+$	+0.6		Extrapolation	[65]
^{24}Mg	0^+	+0.61(5)		BCSM, 38 MeV	[65]
		+0.68(4)		BCSM, 50.5 MeV	[65]
		+0.47		(p,p')	[81]
		+0.45		(c,c')	[80]
		(0.3÷0.7)		Var. exp. meth.	[62]
			+0.46	Hartree–Fock	[71–73]
			+0.26	Variational	[74–76]
			+(0.44−0.47)	K harmonics	[77–82]
^{25}Mg	$5/2^+$	+0.47		Calculated from Q	[53]
^{26}Mg	0^+		+0.19	Hartree–Fock	[83]
^{27}Mg	$1/2^+$	+0.22		Calculated from Q	[62]
^{28}Mg	0^+	+0.2		Extrapolation	[65]

$$|C_1(2)| = \frac{2}{3}\sqrt{\frac{\pi}{10}}\frac{\alpha^{-2}}{\omega^{1/2}AR_0}\left[\sum_{(jj')_\xi=n,p}\frac{N_{jj'}}{[(E_j+E_{j'})^2-\omega^2]^2}\right]^{-1/2} \times \sum_{(j_1j_2)_\xi=n,p}\frac{q_{\text{eff}}^{\xi}N_{j_1j_2}}{(E_{j_1}+E_{j_2})^2-\omega^2}, \quad (28)$$

where

$$N_{j_1j_2}=(2j_1+1)(2j_2+1)(U_{j_1}V_{j_2}+U_{j_2}V_{j_1})^2 \times\langle j_1|r^2|j_2\rangle^2(j_1\,j_2\,\tfrac{1}{2}-\tfrac{1}{2}|20)^2(E_{j_1}+E_{j_2}),$$

$E_j=[(\epsilon_j-\lambda)^2+\Delta^2]^{1/2}$ is the quasiparticle energy, $U_j^2=\frac{1}{2}[1+(\epsilon_j-\lambda)/E_j]$, $V_j^2=\frac{1}{2}[1-(\epsilon_j-\lambda)/E_j]$ are the functions of a Bogolyubov canonical transformation, and they satisfy $U_j^2+V_j^2=1$; $\langle j_1|r^2|j_2\rangle$ is the radial matrix element, $(j_1j_2\frac{1}{2}-\frac{1}{2}|20)$ is a Clebsch–Gordan coefficient, $R_0=1.2A^{1/3}$, ω is the energy of the collective 2^+ level, which is important for the further exposition; j is the total angular momentum of a nucleon in the (n,l)th nuclear shell, N is the principal quantum number, l is the orbital angular momentum of the nucleon, $\alpha=(m\omega_0/\hbar)^{1/2}$ is an oscillator parameter with $\hbar\omega_0=41A^{-1/3}$ MeV, m is the nucleon mass, and $(U_{j_1}V_{j_2}+V_{j_1}U_{j_2})^2=U_{j_1}^2V_{j_2}^2+U_{j_2}^2V_{j_1}^2+\frac{1}{2}\Delta^2/E_{j_1}E_{j_2}$. The summation in both sums in (28) is over the states of similar nucleons in the nuclear shell, i.e., over states of proton–proton and neutron–neutron pairs in the outer open shells of the nucleus. The values of the parameters needed for the calculations are given in Tables VII–XVI of Ref. 52, and the single-particle energies within each shell are found in accordance with the formulas of Appendix II of the same study:

$$\epsilon_j(A)=\epsilon_j^0(A_0)\left(\frac{A_0}{A}\right)^{1/3}+\alpha_j\left(\frac{A_0}{A}\right)^{2/3}$$
$$\times\left[1-\left(\frac{A_0}{A}\right)^{1/2}\right]+\Delta\varepsilon_j(Z,N), \tag{29}$$

where the values of $\epsilon_j^0(A_0)$ for some chosen A_0 are given in the tables. Also given there are the shifts $\Delta\varepsilon_j(Z,N)$. If both levels $j=l\pm 1/2$ are present in the shells, then

$$\alpha_{l\pm 1/2}=\mp[\epsilon_{l-1/2}^0(A_0)-\epsilon_{l-1/2}^0(A_0)]\frac{l'}{2l+1}, \tag{30}$$

$l'=l$ for $l+1/2$ and $l'=l+1$ for $l-1/2$. If there is only one level with $j=1+1/2$ or $j=1-1/2$ present in the shell, then

$$\alpha_{l\pm 1/2}=\mp 7A_0^{-2/3}l'. \tag{31}$$

The single-particle energy levels of the Nilsson potential were used in the calculation, and the chemical poten tials $\lambda_{p,n}$ and the energy gap $\Delta_{p,n}$ were taken from Ref. 52. The radial matrix elements were calculated in accordance with the formulas of the harmonic-oscillator model given in Ref. 48. As energies ω, we took the experimental energies of 2^+ collective levels.[53–55]

Figure 3 gives the results of calculations and a comparison with experiment. Also found were the optimum values of the effective mass proton and neutron charges q_{eff}^p and q_{eff}^n corresponding to the minimum rms deviation of the theoretical $|C_1(2)|$ from their experimental values:

$$q_{\text{opt}}^p=3.10,\ q_{\text{opt}}^n=1.38. \tag{32}$$

It can be seen from Fig. 3 that on the basis of the superfluid model the experimental data on inelastic scattering of α particles at medium energies can be satisfactorily explained for a large number of nuclei.

In the second calculation, we used expressions that do not contain the effective charges:[51]

$$|C_1(2)|=\frac{4\pi}{3\sqrt{5}}\frac{1}{AR_0}\frac{\hbar}{m\omega_0}\frac{S_2^p(\omega)+S_2^n(\omega)}{(S_2'^p(\omega)+S_2'^n(\omega))^{1/2}}, \tag{33}$$

where

$$S_2(\omega)=\frac{1}{4\pi}\sum_{jj'}\frac{(2j+1)(2j'+1)(jj'1/2-1/2|20)^2(N'l'|r^2|Nl)^2(U_jV_{j'}+U_{j'}V_j)^2(E_j+E_{j'})}{(E_j+E_{j'})^2-\omega^2},$$
$$S_2'(\omega)=\frac{1}{4\pi}\sum_{jj'}\frac{\omega(2j+1)(2j'+1)(jj'1/2-1/2|20)^2(N'l'|r^2|Nl)^2(U_jV_{j'}+U_{j'}V_j)^2(E_j+E_{j'})}{[(E_j+E_{j'})^2-\omega^2]^2}. \tag{34}$$

Here, $S_2(\omega)$ and $S_2'(\omega)$ have the form

$$S_2(\omega)=S_2^{(1)}(\omega)+S_2^{(2)}(\omega),$$
$$S_2'(\omega)=S_2'^{(1)}(\omega)+S_2'^{(2)}(\omega), \tag{35}$$

where $S_2^{(1)}(\omega)$ and $S_2'^{(1)}(\omega)$ contain sums over all pairs of nucleons in the nuclear cloud, i.e., they are calculated in exactly the same way as before, when only the nucleons of the outer open shells were taken into account (33). The

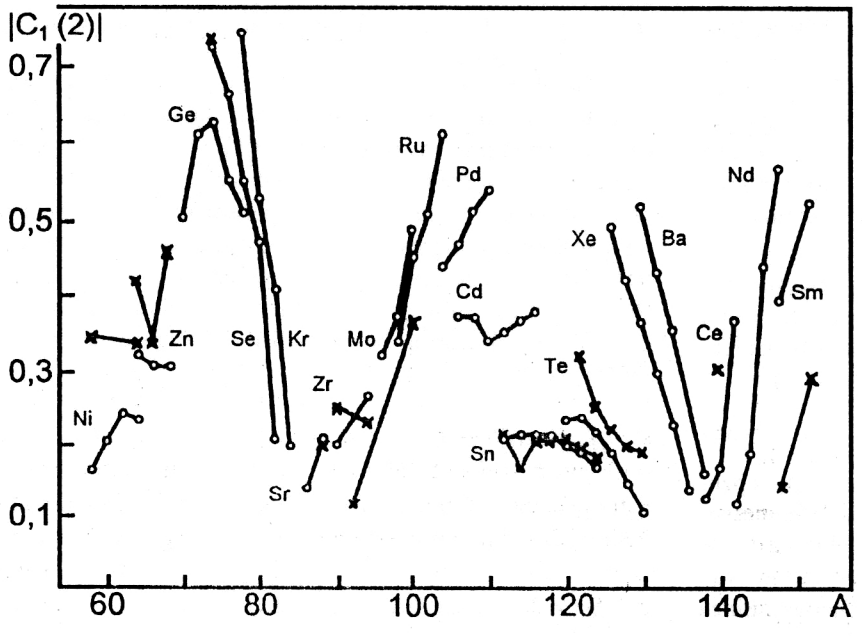

FIG. 3. Comparison of experimental and theoretical values of the nuclear matrix elements $|C_1(2)|$. The crosses represent experiments, and the open circles are for the theory.

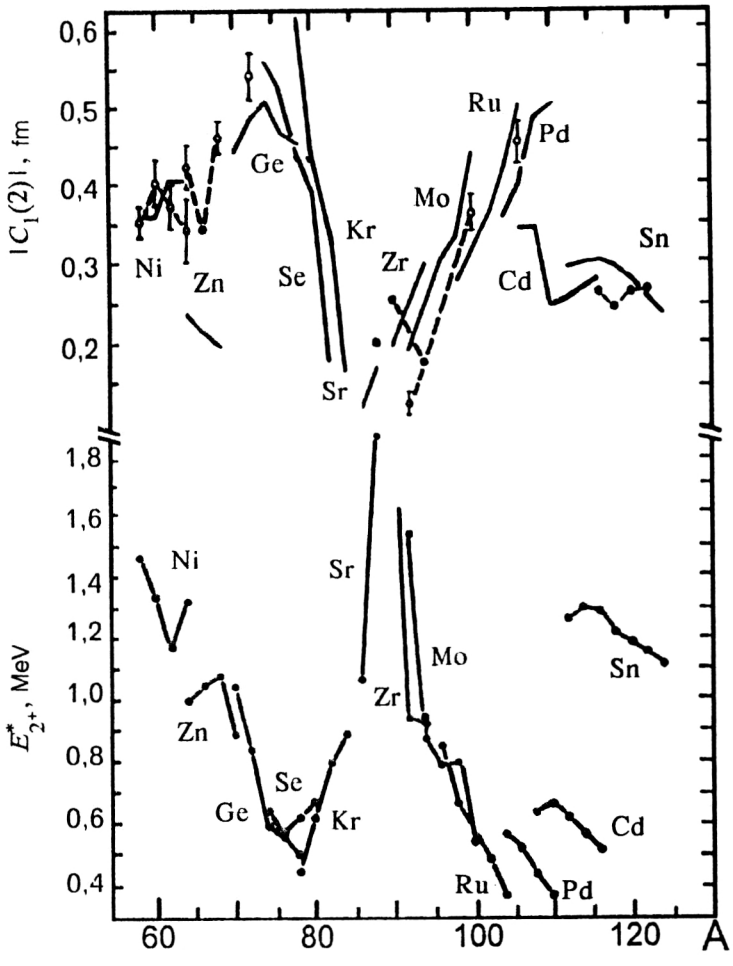

FIG. 4. Calculation of nuclear matrix elements in the superfluid model without introduction of effective mass charges and comparison with energies of 2^+ levels. The black circles represent experiments, and the broken lines are for the theory.

interaction of quadrupole–quadrupole type in closed shells is taken into account, not by the effective charges q^ξ, but by the terms $S_2^{(2)}(\omega)$ and $S_2'^{(2)}(\omega)$ in (35).

Using Eq. (33), we calculated $C_1(2)_{\text{theor}}$, the results of which are shown in Fig. 4 and compared with experimental data.[51] These results again confirm that the microscopic model correctly describes the matrix elements for a large number of nuclei, and, with them, the nuclear deformation parameters. In addition, from Fig. 4 one can see the functional anticorrelation of $C_1(2)=f(A)$ and $E^*_{2+}=f(A)$, this being observed both in general, over the complete range of mass numbers, as well as from isotope to isotope within a given Z of the nuclei. In particular, in the region of $A=75$ and 110 one observes maxima in the function $C_1(2)=f(A)$ and minima in the function $E^*_{2+}=f(A)$.

There follows from Eqs. (28)–(35) a remarkable relation between the nuclear matrix elements and, therefore, the nuclear deformation parameters β_2 and the experimentally well-measured energy E^*_{2+} of the first 2^+ level:

$$\beta_2=1/(E^*_{2+})^{1/2}. \tag{36}$$

This relation suggested the use of this basic energy dependence of the superfluid model to calculate the phenomenological parameters $\beta_2(Z,N)$ for all nuclei, including those for which there are no measurements of the deformation parameters but the energy of the 2^+ level is known. Since the values of E^*_{2+} are known not only for all stable even–even nuclei but also for a large number of radioactive nuclei, the number of such values of $\beta_2(Z,N)$ is much greater than the reserve of experimental deformation parameters measured experimentally through the nuclear matrix elements, probabilities of electromagnetic transitions, widths, and other primary experimental parameters, which are then converted to nuclear deformation parameters using one of the models.

Therefore, on the basis of our proposed phenomenological calculation of $\beta_2(Z,N)$ in accordance with (36) we can construct and investigate the $\beta_2(Z,N)$ surface and its features. To ensure that such calculations are realistic, and to avoid the use of numerous free parameters of the theory, we considered it necessary in calculating the absolute values of $\beta_2(Z,N)$ to normalize in each of the isotopic chains the theoretical value β_2^{theor} to the experimental value for one of the isotopes best studied in the experiments ($\beta_2^{\text{exp}}=\beta_{\text{ref}}$):

$$\beta_2^{\text{theor}}=\beta_2^{\text{exp}}\equiv\beta_{\text{ref}}, \tag{37}$$

calling it the reference value. Then from (36) we readily obtain the final expression for the practical calculations:

$$\beta_2(Z,N)=\beta_{\text{ref}}(Z,N_{\text{ref}})(E_{\text{ref}}/E_2)^{1/2}. \tag{38}$$

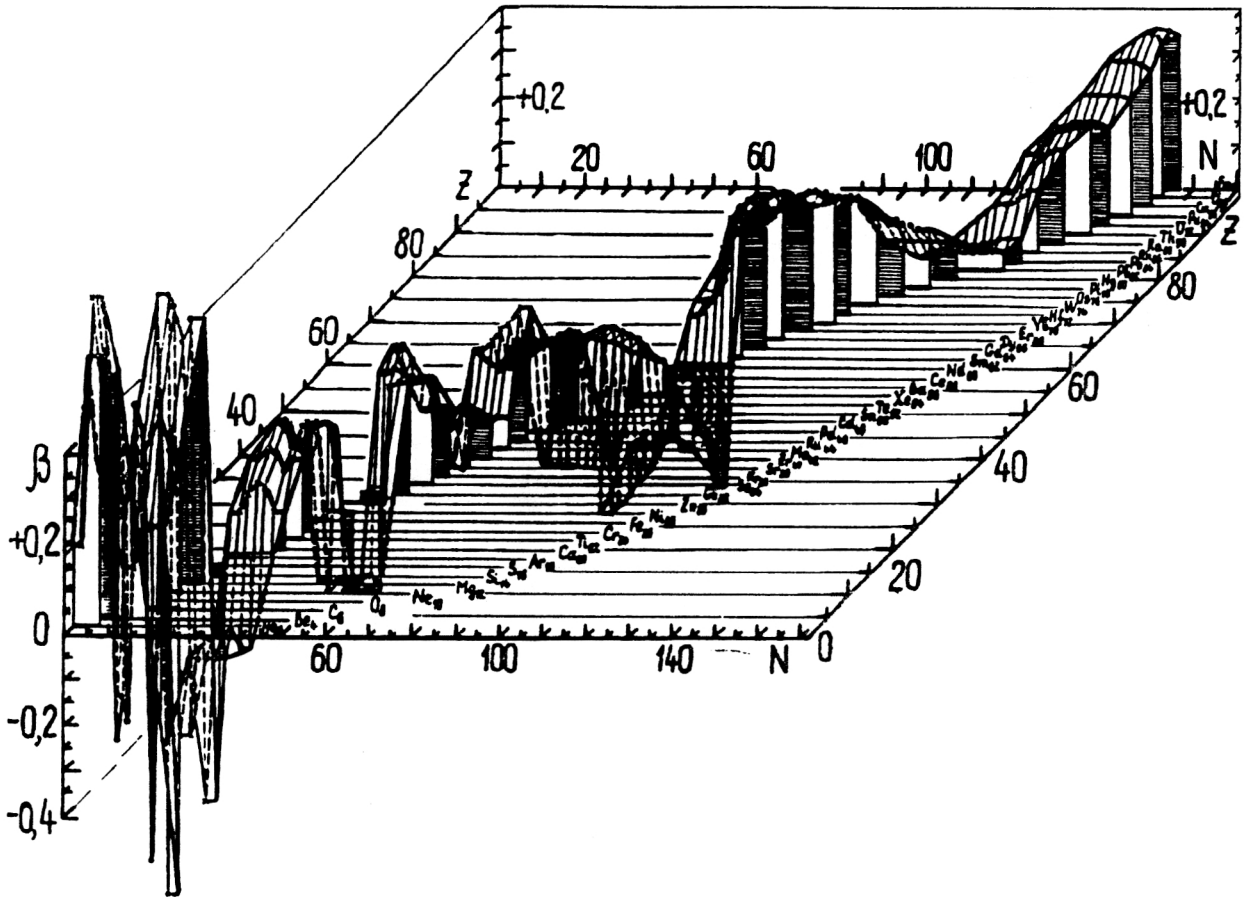

FIG. 5. The nuclear deformation surface $\beta(Z,N)$.

Table IV gives the results of calculations in accordance with Eq. (38) in a comparison with the available systematizations and the experimental data. Moreover, using the coupled-channel method and the Blair phase-shift method, we have reconstructed for the first time the $\beta_2(Z,N)$ surface together with the signs of the nuclear deformation. The signs were chosen on the basis of experimental data and, when they were not available, theoretical calculations.

Figure 5 shows the complete surface $\beta_2(Z,N)$ obtained in the manner described above, together with the signs of the deformation parameters. We now analyze the features of this surface, dividing it nominally into the ranges of light ($Z=2$–28), medium ($Z=28$–50), and heavy ($Z=50$–102) nuclei.

Deformation surface of light nuclei with $Z=2$–28

The above calculations of the shape of light nuclei with large neutron excess in conjunction with the available experimental data enable us to trace the variations in the shape of the nuclear surface from isotope to isotope, and also for other nuclei as functions of Z [of course, if the surface $\beta(Z,N)$ is available, one can consider any other sections of this surface]. Figure 5 gives a three-dimensional representation of the nuclear deformation surface $\beta(Z,N)$, including the surface for the range of light nuclei.

Figure 5 reveals the following main trends in the behavior of $\beta(Z,N)$ for the region of light nuclei. The first is the sign variability for the section of the surface $\beta(Z,N)$ through the so-called $4n$ nuclei, where n is the number of α clusters; this property was first noted in our study of Ref. 65. We shall dwell on it below. In connection with the sign alternation of the nuclear deformation in this section for the surface $\beta(Z,N)$ we note the presence of two "valleys" with negative deformations ("valleys" of oblate nuclei): "valley 1" in the region of carbon and "valley 2" in the region of sulfur.

The second property is the presence of deformations of very large absolute magnitude in the form of characteristic "peaks": "peak 1" in the region of the helium–beryllium isotopes, and "peak 2" in the region of magnesium.

The third feature is the fact that the deformation parameter takes characteristic average values with $\beta\sim0.2$ for all remaining nuclei in the region of the "plateau" from titanium to nickel.

Evidently, the general physical reasons for these features are that, beginning with the lightest nuclei, which have a cluster structure consisting of two-, three-, and four-particle clusters, we come to the formation of purely

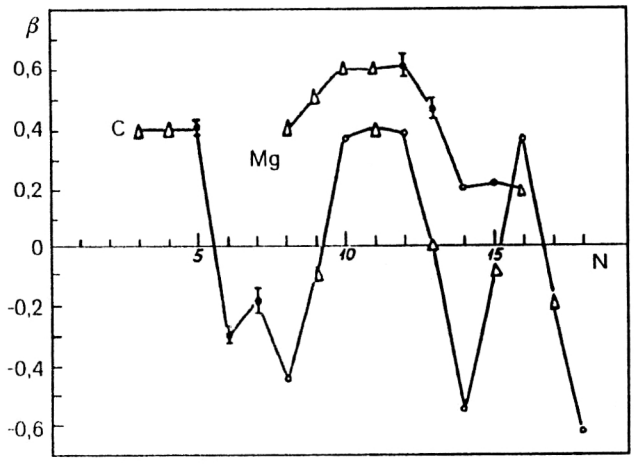

FIG. 6. Change in the shape of the surface of light nuclei as a function of the number of neutrons N (isotopic effects) and the number of protons Z (isotonic effects on the transition from $Z=6$ to $Z=12$). The black circles represent the experiments, the open circles are the theoretical calculations of Refs. 67 and 68, and the open triangles are interpolated and extrapolated values.

α-cluster nuclei, and then, in the region of the "plateau," the formation of a mean field.

We consider the $4n$ dependence in more detail. The reference nuclei here are ^{12}C and ^{24}Mg. From the set of experimental data, partly represented in Table IV, there follows the conclusion that the ^{12}C nucleus is oblate (sign $\beta<0$), while the ^{24}Mg nucleus is prolate (sign $\beta>0$). Comparing these data with the results of theoretical calculations[66–68] (Table VII), we see that great attention has been devoted in the literature to theoretical studies of the shape of the surface of the carbon and magnesium isotopes. It can be seen from Table VII that the main models used to calculate the shapes of the surfaces of light nuclei were: 1) various modifications of the Hartree–Fock method (Ref. 66); 2) the direct variational method of Filippov (Ref. 67); 3) the method of K-harmonic polynomials.[68]

The set of calculated and experimental data make it possible to trace the variation of the nuclear surface on the transition from isotope to isotope (Fig. 6). One can trace the fairly regular, already noted, change in the shape of the nuclei of carbon isotopes as they are enriched with neutrons. Moreover, there are phase transitions of the second kind of nuclei from oblate to prolate shape after the addition of one and then several 4-neutron groups. For the magnesium isotopes, the nuclei have prolate shape, and there are no phase transitions. Nevertheless, for magnesium too one can observe the same tendency for a regular change in the nonsphericity on the addition of 4-neutron groups.

Figure 7 shows the section of the surface $\beta(Z,N)$ through the nuclei with $4n$ structure when an α cluster and not a 4-neutron group is added to the nucleus. As in the case of carbon and magnesium, the shape of the $4n$ nuclei as a function of Z passes from oblate to prolate and back with a similar dependence.

The interpretation of these sign-alternating dependences is of great interest for nuclear theory. Indeed, the jumps in the shape of light nuclei on the addition of $4n$-nucleon structures can be unambiguously interpreted as a direct experimental confirmation of the clustering of light nuclei. There is evidently a simple semiclassical explanation of these new effects in the shapes of light nuclei—they are a manifestation of the individualized existence of intranuclear clusters. The insets in Fig. 7 show a schematic representation of such a $4n$-cluster structure, which is close to the well-known α model (Ref. 69): Two α clusters give a prolate surface, three an oblate surface, four a spherical surface, five again a prolate surface, and so forth, in accordance with Figs. 5–7. It is remarkable that this $4n$-cluster behavior of the shape is observed both in Z and in N.

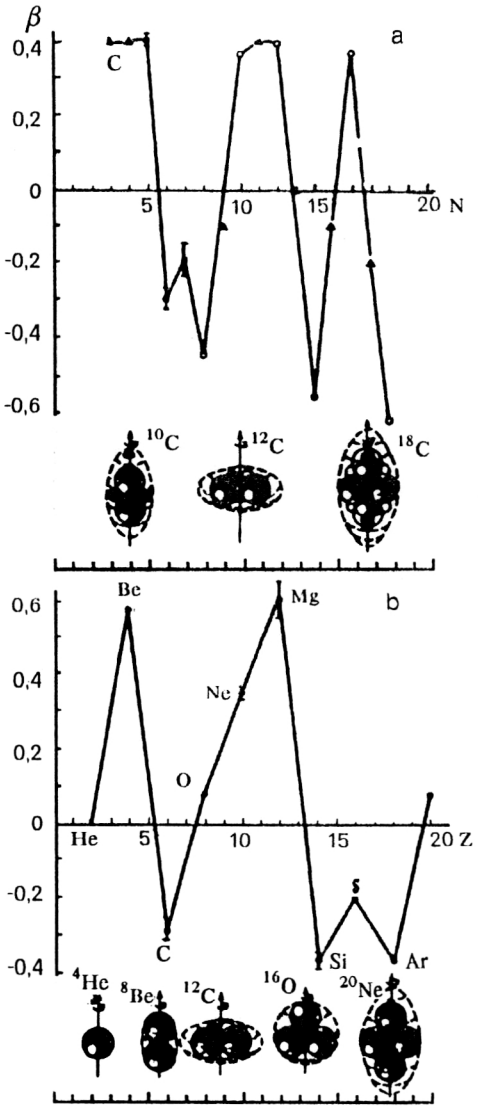

FIG. 7. Cluster effect in the shape of light nuclei: a) change in the shape of nuclei in the isotopic series of carbon on the addition of neutron pairs; b) change in the shape of the α-cluster $4n$ nuclei. The black circles represent the experiments, the open circles are the calculation of Ref. 89, and the black triangles are interpolated and extrapolated values.

Deformation surface of medium nuclei with $Z=28$–50

In Fig. 5 and Table IV we also give the surface $\beta(Z,N)$ for the region $Z=28$–50. It can be seen that it possesses a number of features having a global nature: There are two valleys with oblate nuclei, although oblate nuclei are a rare phenomenon in nuclear physics, in the region of Zn–Ge and Sn–Ba; there is one valley of spherical nuclei in the region of molybdenum, which is situated between the valleys of oblate nuclei; finally, between these three valleys there are elevations with typical Bohr–Mottelson nuclei like krypton and palladium.

In the individual shape of the surface of the isotopes of the medium nuclei in the range $Z=28$–50 one can recognize a trend different from that of the light nuclei, namely, the nuclear shape changes from prolate to oblate only for the semimagic series of nickel isotopes on each addition of a pair of nucleons. In the other isotopic series, the shape of the nuclei either passes smoothly from prolate to oblate, as for the germanium isotopes, or is simply oblate for the entire isotopic series, as for the isotopic series of tin. Thus, the characteristic isotopic effect for the shape of the surface of medium nuclei is a smooth change of only the absolute values of the deformation without a change of its sign. As an example, the zinc isotopes $^{64-70}$Zn are a very interesting subject for investigation of nuclear structure, since with changing number of neutrons in the region $N=34$–40 there is a competitive filling of the $f_{5/2}$ and $p_{1/2}$ levels, and in the ^{70}Zn nucleus the f and p shells are completely filled; the number $N=40$, and also 38 and 60 are "magic," in the first case in the harmonic-oscillator model, and in the second for strongly deformed nuclei.[84] Therefore, one would expect anomalies in the isotopic variations of the structure and shape of the zinc nuclei analogous to the anomalies in the total cross sections,[85,86] in the radii of strong absorption,[87] and in the shapes of the surface[30] found for the Fe and Ni nuclei on the closing of the $f_{7/2}$ shell. The isotopic dependence of the experimental parameters associated with the radius R and the surface thickness ΔR of the zinc nuclei, and also with the nuclear matrix elements $|C_1(I)|$ and the deformations β_2 can be seen in Tables I–IV. The observed smooth dependence of the parameters does not confirm the theoretical predictions of special structure of the zinc nuclei, in particular the ^{64}Zn nucleus.[88]

Isotopic sections of the surface $\beta(Z,N)$, i.e., the signs and magnitudes of the deformation parameters for Mo, Zn, and Te isotopic series, are shown in Figs. 5 and 8. As in the region of medium nuclei, the shape here does not undergo abrupt jumps: The Mo isotopes pass from a spherical shape (^{92}Mo) to a strongly deformed prolate shape (^{100}Mo). The shape of the tin isotopes, in contrast, is slightly oblate, and the deformation merely increases on the addition of nucleon pairs. The nuclei of the Te isotopes have prolate shape.

The smooth changes of the deformation in the isotopic series of iron and zinc, as in the heavier nuclei (Mo,Sn,Te), correspond fully to the conclusions of the generalized model. At the same time, the presence of jumps in the shape of the nuclei of the nickel isotopes can only be

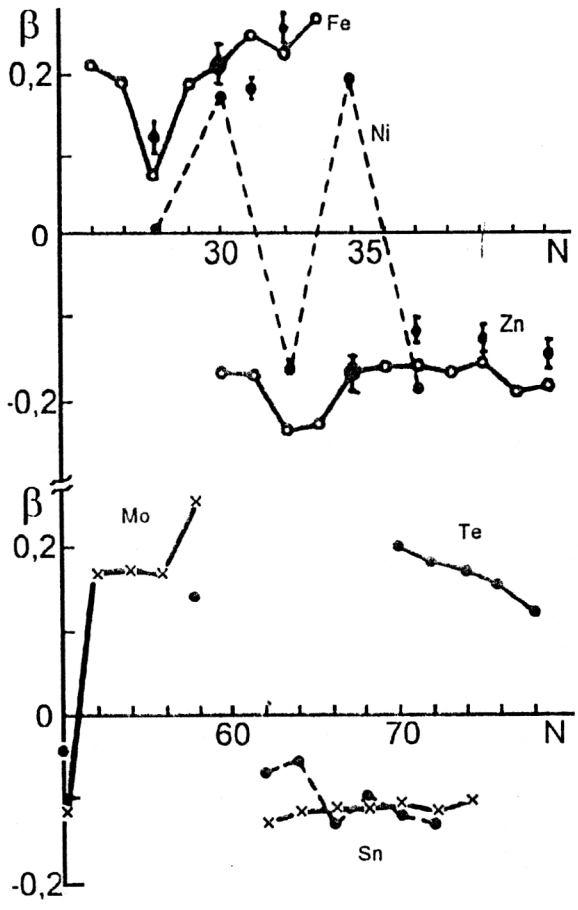

FIG. 8. Changes of the deformation surface $\beta(Z,N)$ in isotopic series for iron, nickel, zinc, molybdenum, tin, and tellurium.

explained under the assumption of a large amplitude of the zero-point vibrations and the magic nature of these nuclei. This corresponds to shell notions, i.e., to a dynamic nature of the equilibrium deformation. The trends found here experimentally are largely confirmed by theoretical calculations in the framework of the variational approach, the method of K harmonics (for light nuclei), and the Hartree–Bogolyubov–Fock method (for medium nuclei) and have a general nature. Similar theoretical predictions for the signs of the deformation of light[89] and heavy[90] nuclei are known. Calculations in the region of medium nuclei with $Z=20$–40 and, in particular, for the even–even isotopes of zinc[91] predict an oblate shape for solution by the Hartree–Bogolyubov–Fock method and a spherical shape for the BCS approximation. Thus, our data agree with the results of solution by the first method.

Deformation surface of heavy nuclei with $Z=50$–102

Heavy nuclei have anomalously large β, especially in the region of the rare earths, and a reliably established rotational nature of the first 2^+ levels; this is important for the experimental determination of the signs of the deformations by the Blair phase-shift method. The development of effective theoretical methods for calculating nuclear

shapes in the framework of microscopic models[92–94] stimulates efforts to create experimental approaches to the solution of this problem, but measurement of only the signs of the electric quadrupole moments is not a complete answer to the problem, since they are sensitive only to the charged component of the nuclei.

It follows from our experiments and analysis of the literature[9] that the data on sign β for heavy nuclei obtained by different methods agree satisfactorily. The investigations (see Table IV) reveal the following general trend in the values of sign β: Whereas in few-nucleon systems (the regions of light and medium nuclei with $A < 100$) the shape of nuclei can change abruptly[30]—the addition of a pair of nucleons may transform a prolate spheroid into an oblate spheroid and vice versa—in many-nucleon heavy nuclei the shape of the surface remains the same within neighboring isotopes. Thus, in the region of heavy nuclei smooth changes in the shape of the surface from nucleus to nucleus are observed.

At the least, our investigation of nuclear shapes by the Blair phase-shift method and by the coupled-channel method enable us to draw the conclusion, valid for the region of heavy nuclei, which has been carefully investigated in experiments, that phase transitions of the second kind are impossible for the shape of the surface of heavy nuclei, especially within the stability valley for isotopic lines.

The $\beta(Z,N)$ surface for heavy nuclei begins with the Sn "valley" of oblate nuclei, which extends up to neodymium. Only at the beginning of this valley is there "cut out" a "crest" of prolate nuclei along two isotopic lines of tellurium and xenon. Then, beginning with the samarium isotopes, there is a rise of the $\beta(Z,N)$ surface to the typical Bohr–Mottelson "plateau" of prolate nuclei with large (up to 0.3–0.4) quadrupole deformation. In the region of lead, this plateau again sinks into the "valley" of the mercury, lead, and polonium isotopic lines, which, however, do not pass through zero and do not acquire prolate shapes. Beginning with radon, there is again formed a plateau of prolate nuclei, which extends with a rise to the boundary of known elements. The new plateau includes very large deformation parameters, and this, in our view, is one of the main physical reasons why there are no stable nuclei in this region. In its turn, the reason for the appearance of large deformation parameters is evidently the competition between the high Coulomb field at large Z and the strong interaction. Thus, it is to be expected that the search for a new stability island will be crowned with success in investigations that find a way of suppressing this competition and, thereby, reducing the deformation parameters of superheavy nuclei.

In the region of heavy nuclei one can clearly trace the general tendency in the isotopic lines of the $\beta(Z,N)$ surface as they move to the edges of the stability tracks. This is, together with the clear regular rise in the deformation at half filling of the subshells and shells, as described by the generalized model, the presence of a general tendency for the deformation to increase with both increasing neutron deficit and neutron excess. Evidently, the nuclear instability not only in Z, as noted above for the transuranium nuclei, but also in N can be explained by the growth of the nuclear deformation.

The establishment of the new interesting trends in the surface $\beta(Z,N)$ confirms once more the topicality of measuring the $E^*_{2^+}$ energies at the edges of the stability tracks along the Z lines too, and also direct measurements of the parameters β and sign β for the isotopic and isotonic lines. It is also obviously topical to investigate of the ratios of the Coulomb and nuclear fields for large and maximal Z, and also their interference in these regions of nuclear masses and charges.

CONCLUSIONS

From experimental data on the scattering of α particles of medium energies (20–140 MeV), using the coupled-channel method and the Blair phase-shift method, we have extracted experimental values of the nuclear quadrupole deformation parameter $\beta(Z,N)$ and its sign, sign $\beta(Z,N)$, in the region $Z=2$–102 and compared them with the available experimental and theoretical literature data.

Our comparison with theoretical calculations in the framework of a superfluid model suggested the use of the basic energy dependence $\beta \sim 1/E^{*1/2}_{2^+}$, where $E^*_{2^+}$ is the energy of the first 2^+ level, to calculate semiempirical deformation parameters for the nuclei for which experimental data on β or theoretical calculations of them are not available. Since the values of $E^*_{2^+}$ are known not only for all stable nuclei but also for a large number of radioactive even–even nuclei, the number of $\beta(Z,N)$ values that we were able to obtain is much greater than the number of direct experimental data. On the basis of this resource of data, we have constructed and investigated the surface $\beta(Z,N)$. We have found numerous new features.

First, we have found that oblate nuclei are a rare phenomenon in nuclear physics, although five "valleys" of oblate nuclei have been established more or less reliably: in the region of carbon, silicon–sulfur, nickel–zinc, tin, and neodymium–barium. It is also interesting to note an incipient sixth "valley" in the region of lead, but the deformation "does not stretch" to oblate shapes, or it has not yet been detected.

Second, in the surface $\beta(Z,N)$ there are fairly high "peaks," large "elevations," and extended "plateaux" of the nuclear deformation. The "peaks" are observed for the Be and Mg isotopes; the "elevations" for the regions Cr–Ti and Ge–Sr; and the Bohr–Mottelson "plateaux" of prolate nuclei in the region of tellurium, from samarium to platinum, and beyond radium.

Third, since the reconstructed surface $\beta(Z,N)$ still does not yet encompass all nuclei discovered up to the present time, simple measurements of the energy of the first 2^+ level for distant and transuranium nuclei become very topical. Finally, the discovered growth of the deformation at the edges of the stability tracks and at large known Z offers hope that the physical reason for the finiteness of the periodic table and instability of nuclei has been understood, and at the edges of the stability track one can

expect the occurrence of nuclei with superdeformation or with exotic shape.

[1] V. G. Soloviev, *Nuclear Theory. Nuclear Models* [in Russian] (Énergoizdat, Moscow, 1981).
[2] *Problems of Modern Nuclear Physics*, edited by V. M. Kolybasov [in Russian] (Nauka, Moscow, 1971).
[3] E. Rutherford, Philos. Mag. **21**, 669 (1911).
[4] R. Hofstadter, *Electron Scattering and Nuclear and Nucleon Structure* (Benjamin, New York, 1963).
[5] A. Bohr, K. Dan. Vidensk. Selsk. Mat.-Fys. Medd. **26**, No. 14 (1952).
[6] A. Bohr and B. Mottelson, K. Dan. Vidensk. Selsk. Mat.-Fys. Medd. **27**, No. 16 (1953).
[7] V. G. Nosov, Zh. Eksp. Teor. Fiz. **53**, 579 (1967) [Sov. Phys. JETP **26**, 375 (1968)].
[8] D. A. Arsen'ev, V. V. Pashkevich, V. G. Solov'ev, and U. M. Faĭner, Preprint R4-6587 [in Russian], JINR, Dubna (1972).
[9] A. V. Yushkov, Izv. Akad. Nauk SSSR, Ser. Fiz. **39**, 1584 (1975).
[10] E. V. Inoshin and A. V. Shebeko, Zh. Eksp. Teor. Fiz. **51**, 1761 (1966) [Sov. Phys. JETP **24**, 1189 (1967)].
[11] A. I. Akhiezer and I. Ya. Pomeranchuk, *Some Problems of Nuclear Theory* [in Russian] (Gostekhizdat, Moscow–Leningrad, 1950).
[12] E. V. Inopin, Zh. Eksp. Teor. Fiz. **50**, 1592 (1966) [Sov. Phys. JETP **23**, 1061 (1966)].
[13] V. Yu. Gonchar, K. S. Zheltonog, and A. V. Yushkov, Izv. Akad. Nauk Kaz. SSR, Ser. Fiz.-Mat. **6**, 3 (1969).
[14] L. R. B. Elton, *Nuclear Sizes* (Oxford University Press, London, 1971) [Russ. transl., IIL, Moscow, 1962].
[15] D. I. Blokhintsev, *Fundamentals of Quantum Mechanics* [in Russian] (Vysshaya Shkolya, Moscow, 1963).
[16] B. I. Tishchenko and E. V. Inopin, Yad. Fiz. **7**, 1029 (1968) [Sov. J. Nucl. Phys. **7**, 618 (1968)].
[17] S. Ya. Aĭsina, K. A. Kuterbekov, V. N. Tolstikov *et al.*, Preprint 2–87 [in Russian], Institute of Nuclear Physics, Kazakh Academy of Sciences, Alma-Ata (1987).
[18] R. S. Nataf, *Les Modèles en Spectroscopie Nucléaire* (Paris, 1963) [Russ. transl., Mir, Moscow, 1968].
[19] N. N. Pavlova, S. Ya. Aĭsina, K. A. Kuterbekov *et al.*, Preprint [in Russian], Institute of Nuclear Physics, Kazazh Academy of Sciences, Alma-Ata (1990).
[20] S. Ya. Aĭsina, K. A. Kuterbekov, N. N. Pavlova, and A. V. Yushkov, Preprint 13–84 [in Russian], Institute of Nuclear Physics, Kazakh Academy of Sciences, Alma-Ata (1984).
[21] K. S. Zheltonog, *Candidate's Dissertation* [in Russian] (Alma-Ata, 1971).
[22] K. A. Kuterbekov and A. V. Yushkov, Izv. Akad. Nauk SSSR, Ser. Fiz. **53**, 2098 (1989).
[23] K. A. Kuterbekov, S. Ya. Aĭsina, N. N. Pavlova, and A. V. Yushkov, Preprint [in Russian], Institute of Nuclear Physics, Kazakh Academy of Sciences, Alma-Ata (1991).
[24] A. V. Yushkov, *Doctoral Dissertation* [in Russian] (Alma-Ata, 1991).
[25] V. Yu. Gonchar, K. S. Zheltonog, G. N. Ivanov, and A. V. Yushkov, Yad. Fiz. **8**, 678 (1968) [Sov. J. Nucl. Phys. **8**, 393 (1969)].
[26] E. V. Inopin, Izv. Akad. Nauk Kaz. SSSR, Ser. Fiz.-Mat. **6**, 28 (1972).
[27] T. Tamura, Rev. Mod. Phys. **37**, 679 (1963).
[28] J. Raynal, *Computing as a Language of Physics* (IAEA-SMR 918), p. 281; *The Structure of Nuclei* (IAEA 8/8), p. 75.
[29] I. N. Kukhtina, N. N. Pavlova, and A. V. Yushkov, Izv. Akad. Nauk SSSR, Ser. Fiz. **55**, 2265 (1991).
[30] V. Yu. Gonchar and A. V. Yushkov, Izv. Akad. Nauk SSSR, Ser. Fiz. **35**, 830 (1971).
[31] G. D. Alkhazov, Preprint 599 [in Russian], Leningrad Institute of Nuclear Physics (1980).
[32] I. I. Zalyubovskiĭ and P. M. Gonych, *Nuclear Spectroscopy* [in Russian] (Vyshcha Shkola, Khar'kov 1980).
[33] E. V. Inopin, *Doctoral Dissertation* [in Russian] (Khar'kov 1967).
[34] S. Raman, C. W. Nestor, Jr., S. Kahane, and K. H. Bhatt, At. Data Nucl. Data Tables **41**, No. 3 (1989).
[35] Rapp. CEA No. 3147, edited by G. Bruge (1967).
[36] V. V. Alekseev *et al.*, Izv. Akad. Nauk SSSR, Ser. Fiz. **32**, 570 (1968).
[37] K. P. Artemov, V. Z. Gol'dberg, and V. P. Rudakov, Yad. Fiz. **9**, 266 (1969) [Sov. J. Nucl. Phys. **9**, 157 (1969)].
[38] R. K. Jolly, M. D. Goldberg, and A. K. Sengupta, Nucl. Phys. **A123**, 54 (1969).
[39] F. Hinterberger, Nucl. Phys. **115**, 570 (1968).
[40] V. E. Lewis *et al.*, Nucl. Phys. **A117**, 673 (1968).
[41] V. D. Afanas'ev, *Author's Abstract of Dissertation* [in Russian] (Khar'kov, 1969).
[42] Nuclear Structure, edited by V. P. Rudakov [in Russian] (Atomizdat, Moscow, 1962).
[43] A. S. Davydov, *Collective Excitations of Even Nuclei* [in Russian] (Kiev, 1967).
[44] *Direct Processes in Nuclear Reactions* [in Russian], edited by A. A. Ogloblin (Atomizdat, Moscow, 1965).
[45] D. A. Arseniev, A. Sobiczewski, and V. G. Soloviev, Nucl. Phys. **A126**, 15 (1969).
[46] V. Yu. Gonchar, E. V. Inopin, and S. P. Tsytko, Preprint D-001 [in Russian], Khar'kov (1959).
[47] E. V. Inopin and Yu. P. Mel'nik, Yad. Fiz. **9**, 982 (1969) [Sov. J. Nucl. Phys. **9**, 575 (1969)].
[48] *Deformation of Nuclei*, edited by L. A. Sliv [Russian translation] (IIL, Moscow, 1958).
[49] J. S. Blair, Phys. Rev. **115**, 928 (1959).
[50] V. Yu. Gonchar and A. V. Yushkov, Yad. Fiz. **11**, 1034 (1970) [Sov. J. Nucl. Phys. **11**, 574 (1970)].
[51] V. Yu. Gonchar, E. V. Inopin, Yu. P. Mel'nik, and A. V. Yushkov, Izv. Akad. Nauk Kaz. SSR, Ser. Fiz.-Mat. **6**, 77 (1972).
[52] L. S. Kisslinger and R. A. Sorensen, Rev. Mod. Phys. **35**, 853 (1963).
[53] B. S. Dzhelepov and L. K. Peker, *Decay Schemes of Radioactive Nuclei. $A > 100$* [in Russian] (Nauka, Moscow–Leningrad, 1966).
[54] B. S. Dzhelepov, L. K. Peker, and V. O. Sergeev, *Decay Schemes of Radioactive Nuclei. $A < 100$* (USSR Academy of Sciences, Moscow–Leningrad, 1963).
[55] *Table of Isotopes*, edited by C. M. Lederer *et al.* (Wiley, New York, 1978).
[56] Annual Progress Report, Univ. of Washington, June 1962, July 1964, June 1965, June 1966, June 1967.
[57] J. Kokame, K. Fukunaga, H. Nakamura, and N. Inone, J. Phys. Soc. Jpn. **20**, 475 (1965).
[58] H. W. Brock, Phys. Rev. **130**, 1914 (1963).
[59] E. J. Martens and A. M. Bernstein, Nucl. Phys. **A117**, 241 (1968).
[60] O. F. Nemets and Yu. V. Gofman, *Handbook of Nuclear Physics* [in Russian] (Naukova Dumka, Kiev, 1975).
[61] P. E. Hodgson, *The Optical Model of Elastic Scattering* (Oxford University Press, 1963) [Russ. transl., Atomizdat, Moscow, 1966].
[62] É. V. Lan'ko, G. S. Dombrovskaya, and Yu. K. Shubnyĭ, *Probabilities of Electromagnetic Transitions of Nuclei with $Z = 1$–30* [in Russian] (Nauka, Leningrad, 1972).
[63] M. P. Avotina and A. V. Zolotavin, *Moments of Ground and Excited Nuclear States*, Part 1 [in Russian] (Atomizdat, Moscow, 1979).
[64] M. P. Avotina and A. V. Zolotavin, *Moments of Ground and Excited Nuclear States*, Part 2 [in Russian] (Atomizdat, Moscow, 1979).
[65] N. N. Pavlova and A. V. Yushkov, Yad. Fiz. **23**, 252 (1976) [Sov. J. Nucl. Phys. **23**, 131 (1976)].
[66] E. Caurier, B. Bourotte-Bilwes, and Y. Abgrall, Phys. Lett. **44B**, 411 (1973).
[67] A. I. Steshenko and G. F. Filippov, Yad. Fiz. **14**, 715 (1971) [Sov. J. Nucl. Phys. **14**, 403 (1972)].
[68] Yu. T. Grin' and A. B. Kochetov, Yad. Fiz. **18**, 283 (1973) [Sov. J. Nucl. Phys. **18**, 145 (1974)].
[69] V. G. Neudachin and Yu. F. Smirnov, *Nucleon Associations in Light Nuclei* [in Russian] (Nauka, Moscow, 1969).
[70] J. Specht, C. W. Schweimer, H. Rebet, and C. Schatz, Nucl. Phys. **A171**, 65 (1971).
[71] Y. Abgrall, B. Morand, and E. Caurier, Nucl. Phys. **A192**, 372 (1972).
[72] A. L. Goodman, C. L. Struble, and A. Goswami, Phys. Lett. **26B**, 260 (1968).
[73] F. R. Ruchl, Jr., Indian J. Phys. **45**, 149 (1971).
[74] G. F. Filippov, Fiz. Elem. Chastits At. Yadra **4**, 992 (1973) [Sov. J. Part. Nucl. **4**, 405 (1973)].
[75] G. F. Filippov and A. I. Steshenko, Ukr. Fiz. Zh. **15**, 626 (1970).
[76] G. F. Filippov and V. M. Maksimenko, Ukr. Fiz. Zh. **15**, 1277 (1970).
[77] A. I. Baz', Yu. T. Grin', V. F. Demin, and M. V. Zhukov, Fiz. Elem. Chastits At. Yadra **3**, 275 (1972) [Sov. J. Part. Nucl. **3**, 137 (1972)].
[78] Yu. T. Grin', Yad. Fiz. **12**, 927 (1970) [Sov. J. Nucl. Phys. **12**, 506 (1971)].
[79] Yu. T. Grin' and A. B. Kochetov, Yad. Fiz. **12**, 1154 (1970) [Sov. J. Nucl. Phys. **12**, 634 (1971)].

[80]Yu. T. Grin' and L. B. Levinson, Yad. Fiz. **14**, 536 (1971) [Sov. J. Nucl. Phys. **14**, 300 (1972)].
[81]Yu. T. Grin', A. B. Kochetov, and A. I. Anan'kin, Yad. Fiz. **14**, 953 (1971) [Sov. J. Nucl. Phys. **14**, 534 (1972)].
[82]Yu. T. Grin', Pis'ma Zh. Eksp. Teor. Fiz. **20**, 507 (1974) [JETP Lett. **20**, 231 (1974)].
[83]D. H. Kurath, Phys. Rev. C **5**, 768 (1972).
[84]J. H. Hamilton, Lect. Notes Phys. 168 (1982); *Heavy-Ion Collisions. Proc. of the Intern. Summer School* (Rabida, 1982), p. 287.
[85]B. D. Wilkins and G. Igo, Phys. Rev. **129**, 2198 (1963).
[86]G. Igo and B. D. Wilkins, Phys. Rev. **131**, 1251 (1964).
[87]V. Yu. Gonchar and K. S. Zheltonog, Izv. Akad. Nauk Kaz. SSR, Ser. Fiz.- Mat. **2**, 62 (1971).
[88]E. V. Inopin, V. I. Tishchenko, and A. V. Shebeko, Zh. Eksp. Teor. Fiz. **49**, 1824 (1965) [Sov. Phys. JETP **22**, 1247 (1966)].
[89]G. F. Filippov, Fiz. Elem. Chastits At. Yadra **2**, 315 (1971) [Sov. J. Part. Nucl. **2**, No. 2, 19 (1971)].
[90]D. A. Arsen'ev, V. V. Pashkevich, V. G. Solov'ev, and U. M. Faĭner, Preprint R4-6587 [in Russian], JINR, Dubna (1972).
[91]H. Chandra and M. L. Rustgi, Phys. Rev. C **4**, 874 (1971).
[92]D. A. Arsen'ev, V. V. Pashkevich, V. G. Solov'ev, and S. I. Felotov, Preprint R4-6345 [in Russian], JINR, Dubna (1972).
[93]G. F. Filippov, in *Program and Abstracts of Papers at the 21st Symposium on Nuclear Spectroscopy and Nuclear Structure*, Vol. 1 [in Russian] (Nauka, Leningrad, 1971), p. 22.
[94]N. E. Kirikashvili, K. O. Menteshashvili, and V. A. Nabichvrishvili, Soobshch. Akad. Nauk Gruz. SSR **64**, 41 (1971).

Translated by Julian B. Barbour